LIQUID SIDE FLOW CHARACTERISTICS IN A PACKED ABSORPTION COLUMN

by

A.W. BRYSON.

Submitted for the Degree of Doctor of Philosophy at the University of Cape Town.

December, 1965.

PREFACE.

The work described in this thesis was performed in the Chemical Engineering Department of the University of Cape Town during the period January 1962 to December 1965. The work is original except where stated and no part of the thesis has been submitted at any other University.

The author wishes to express his sincere thanks to Professor A.D. Carr for his assistance and encouragement throughout the course of this work. Thanks are due also to Professor E.T. Woodburn and Dr.J.F. Davidson for many helpful discussions and suggestions.

Signed by candidate

ABSTRACT.

This thesis is primarily concerned with the study of techniques which enable flow conditions in complex geometrical arrangements to be measured and analysed. The liquid side in a packed absorption tower is chosen to illustrate the principles involved.

The analysis of disturbance testing involves the evaluation of the moments of the resulting residence time distribution curves. It has in the past been found that this method often produces misleading results due to the magnification of experimental errors. An improved method of moment analysis is introduced in this work in an attempt to lessen this effect. It is also shown that much more useful information can be obtained by measuring the response to a disturbance at a number of selected positions in the bed rather than a single determination at the outlet from the column.

Two mathematical models are chosen to describe the observed flow situation. The values of their characteristic parameters, as determined from the disturbance testing, are shown to exhibit a number of interesting features which enhance our knowledge of liquid side flow conditions.

Finally, a technique is introduced to study flow behaviour from chemical reaction data. The experimental results obtained are shown to agree very closely with theoretically derived values.

INDEX

APPENDIX 1

APPENDIX 2

LIST OF FIGURES

SECTION I

INTRODUCTION

The effect of liquid side dynamics on the performance of a packed gas absorption column has recently been the subject of numerous investigations[1-9]. In nearly all cases a simplified flow situation has been chosen to interpret observed mass transfer rates. A thorough knowledge of the actual flow conditions existing in such a system is as yet incomplete. This has been due to the complex geometrical nature of the system and the difficulties involved in determining these conditions experimentally. Direct measurement of the velocity profile across the film of liquid as it passes over the packing at a particular point would be difficult enough in itself, whereas a complete knowledge would require this measurement to be performed at all points throughout the bed. It follows, therefore, that a study of the flow behaviour in such a system will have to be approached by indirect measurements.

It would be as well at this stage to discuss the need for an accurate representation of the dynamics of the liquid phase in absorption studies. The rate of gas absorption in a packed bed depends on:

(a) The physical and chemical properties of the gas and liquid. These

properties have been thoroughly investigated for a large number of systems and accurate values are generally available.

(b) The flow conditions existing in both phases.

If the absorption process is liquid side controlling and the column is operated below the loading point, the flow conditions existing in the liquid phase, especially in the neighbourhood of the interface, will be important in determining the rate of mass transfer. Interfacial conditions are as yet not fully understood on account of the problems involved in measuring the extent of the effective interfacial area and the surface flow characteristics. The former has been widely studied[10-13], however, as a number of these results seem to be contradictory[14], their value appears dubious. Even if this quantity could be accurately determined, it is also likely that some sections of the area will be more effective than others, and that the relative contribution to the resistance of mass transfer of the various sections will be dependent on the type of absorption process occurring. This postulate appears to be borne out by the results of Danckwerts and Roberts[15] who discovered that, on the assumption of validity of the "Surface Renewal" model, the effective area for absorption accompanied by reaction in the liquid bulk was higher than that for pure physical absorption.

Original theories assumed that the liquid phase was in ideal plug flow. Based on this, reasonable correlations were obtained for physical absorption[16-19]; however, for absorption accompanied by reaction in the liquid phase, the position is not as clear. Apart from the above-mentioned dependence of absorption rate on the effectiveness of the interfacial area, it can be also shown (see Section 2.81) that the percentage error involved in calcu-

lating the rate constant of a first order absorption process on the assumption of plug flow is proportional to the value of the constant. This would indicate that the faster the absorption process the greater will be the significance of the departure from plug flow behaviour of the liquid side. There is every reason to believe that this trend will be true for all liquid side controlling absorption processes.

With the advent of "Stimulus Response" techniques, whereby the distribution of residence times of a fluid in a system could be determined experimentally, new light was thrown on the dynamic behaviour of the liquid phase. However, as this technique describes only the varying ages of the elements of fluid, it can only be applied to rate processes which are dependent on this factor alone. This limitation will, of course, rule out its direct application to many absorption processes. If the rate of absorption across any element of interface can be written as:

$$\frac{dC}{dt} = k(C_e - C) \qquad (1.1)$$

where k and Ce are constants throughout the bed and C is the concentration in the bulk of the liquid immediately below that element of interface, then a knowledge of the distribution of residence times alone will be sufficient to take into account the deviation from ideal flow conditions which might exist in an actual bed. A few absorption processes have been found to follow equation (1.1); an example being the physical absorption of a pure gas. For all other processes and especially those which depend on chemical reaction mechanisms, the absorption will depend not only on the ages of each element, but on their

environment. This means that the elements of liquid can no longer be regarded as independent entities as they now have an intimate effect on one another. In order to determine absorption rates, therefore, it would be necessary to know exactly where each element resided while it passed through the column. This, of course, would be the ideal situation, but one which would be extremely difficult to determine in practice. It does, however, stress the need for a more detailed understanding of the actual flow conditions.

Due to the expected complexities of these conditions it is necessary from a practical point of view to represent the actual flow pattern by relatively simple mathematical models, which will contain a number of characteristic parameters. The problem then reduces to one of selecting a model which agrees most closely with measured phenomena. There must be some basis on which to judge the degree of fit as well as a procedure of investigation which will qualitatively indicate the structure of the model. The fulfilment of these two factors can be approached in the following manner:

(a) From visual observations and theoretical reasoning, an idea of the basic nature of the model can be obtained.

(b) The form of the moments of the residence time distribution curve for the model can be compared with those from experimentally measured distributions.

(c) Greater details concerning the flow conditions can be obtained by measuring residence time distributions at selected points within the bed.

(d) A second or higher order homogeneous chemical reaction can be performed in the liquid phase, the measured average conversion being compared with that which would be expected if the model held exactly.

The steps just outlined were followed in the present study and the experimental work which follows has been divided into two sections - Section 2, which deals with pulse testing and Section 3 in which chemical reaction runs are analysed.

* * * *

SECTION 2

INVESTIGATION OF FLOW BEHAVIOUR BY DISTURBANCE TECHNIQUES

2.1 APPLICATION OF STIMULUS RESPONSE TECHNIQUES TO FLUID DYNAMICS

Danckwerts[20] has introduced a system of nomenclature, definitions and basic principles for treating non-ideal flow. These will be largely adhered to in this section. The quantity which is of most practical importance is the "external age distribution" function, E(t). This function can be determined experimentally by a number of methods, all of which can be classed as "stimulus response" techniques. The procedure is to disturb the system and to analyse the resulting response. The disturbance can be of many types, the most common being the injection of a tracer material in the form of a pulse[21-23] step[24-25] sinusoidal[26-28] or random signal[29]. In this analysis the pulse will be the only case considered as, in the form of a dirac delta signal, it yields the E(t) function directly and is comparatively easy to realise in practice to a fair degree of accuracy. Even if the latter consideration is significantly in error this type of function is amenable to correction as will be demonstrated in Section 2:22.

2.2 MATHEMATICAL BACKGROUND

2.21 Characterisation of the response of a system to a dirac delta concentration input signal.

It can be shown[30] that E(t) is directly proportional to C(t), where C(t) is the concentration of tracer material in the outlet stream of the system at a time t from the injection of the tracer in the inlet stream. To enable residence time distribution measurements for different systems to be quantitatively compared, it is necessary to choose a number of parameters which will characterize the distributions. Danckwerts[20] chose two quantities which he called "Holdback" and "Segregation". These he defined respectively, as:

$$H = \frac{1}{T_m} \int_0^{T_m} F(t)\,dt \qquad (2.1)$$

where T_m is the mean residence time and

$$F(t) = \int_0^t E(t)\,dt \qquad (2.2)$$

$$\text{and} \quad S = \int_0^{t_c} (1 - e^{-t/T_m})\,dt - \frac{1}{T_m} \int_0^{t_c} F(t)dt \qquad (2.3)$$

$$\text{where} \quad t_c = -T_m \ln \left[1 - F(t_c) \right] \qquad (2.4)$$

The two quantities are measures of the deviations from the two ideal flow conditions, namely plug flow and complete mixing respectively.

In this study it has been decided to use the moments of the distribution curves as a means of characterisation, as these are far more sensitive to small changes in the form of the E(t) curves. Although it is true that the

higher the moment, the greater this sensitivity, it is not advisable to extend the analysis beyond the third moment as small experimental errors may be magnified to such an extent that the results become meaningless. Even for lower moments this is to a degree a drawback and will be the subject of discussion in Section 2.23.

The definition of moments to be used in this work can be written as follows:-

(a) Zero moment, α_0

$$\alpha_0 = \int_0^\infty C(t)\,dt \qquad (2.5)$$

(b) First moment about the origin, i.e. the mean

$$T_m = \frac{1}{\alpha_0} \int_0^\infty t\,C(t)\,dt \qquad (2.6)$$

(c) Second moment about T_m, i.e. the spread

$$T_s^2 = \frac{1}{\alpha_0} \int_0^\infty (t-T_m)^2\,C(t)\,dt \qquad (2.7)$$

(d) Third moment about T_m, i.e. the skew.

$$T_a^3 = \frac{1}{\alpha_0} \int_0^\infty (t - T_m)^3\,C(t)\,dt \qquad (2.8)$$

2.22 System transfer function in terms of the moments of the distribution curve.

The La Place Transformation of a function f(t) is by definition[31] :

$$F(s) = \int_0^\infty e^{-st} f(t)\, dt \qquad (2.9)$$

The dynamic process under consideration can be expressed as a transfer function G(s) on a block diagram with input signal θ_i and output θ_o. If θ_i is a unit dirac delta function

$$\theta_o = C(t) \qquad (2.10)$$

Denoting the transformed signals as $\bar{\theta_i}$ and $\bar{\theta_o}$

$$\bar{\theta_i} = 1 \qquad (2.11)$$

and

$$\bar{\theta_o} = \mathcal{L}\, C(t) = \int_0^\infty e^{-st} C(t)\, dt \qquad (2.12)$$

By block diagram algebra[31] ,

$$\frac{\bar{\theta_o}}{\bar{\theta_i}} = G(s) \qquad (2.13)$$

i.e.

$$G(s) = \bar{\theta_o} = \int_0^\infty e^{-st} C(t)\, dt \qquad (2.14)$$

Expanding e^{-st} as a Maclaurin series

$$G(s) = \alpha_0 - s\,\alpha_1 + \frac{s^2}{2}\alpha_2 - \frac{s^3}{6}\alpha_3 \qquad (2.15)$$

where $$\alpha_0 = \int_0^\infty C(t)\,dt \qquad (2.16)$$

$$\alpha_1 = \int_0^\infty t\,C(t)\,dt \qquad (2.17)$$

$$\alpha_2 = \int_0^\infty t^2\,C(t)\,dt \qquad (2.18)$$

$$\alpha_3 = \int_0^\infty t^3\,C(t)\,dt \qquad (2.19)$$

$$\ln G(s) = \ln \alpha_0 + \ln \left(1 - \frac{\alpha_1}{\alpha_0} s + \frac{\alpha_2}{\alpha_0} \frac{s^2}{2} - \frac{\alpha_3}{\alpha_0} \frac{s^3}{6}\right) \qquad (2.20)$$

Expanding the second term on the right hand side of this equation and rearranging terms in increasing powers of s,

$$\ln G(s) = \ln \alpha_0 - \left(\frac{\alpha_1}{\alpha_0}\right)s + \frac{1}{2}\left\{\frac{\alpha_2}{\alpha_0} - \left(\frac{\alpha_1}{\alpha_0}\right)^2\right\} s^2 - \frac{1}{6}\left\{\frac{\alpha_3}{\alpha_0} - \frac{3\alpha_2\alpha_1}{(\alpha_0)^2} + 2\left(\frac{\alpha_1}{\alpha_0}\right)^3\right\} s^3 \qquad (2.21)$$

From the definitions of T_m, T_s^2 and T_a^3 it follows that:

$$\ln G(s) = \delta - T_m s + \frac{1}{2}T_s^2 s^2 - \frac{1}{6}T_a^3 s^3 \qquad (2.22)$$

If a number of dynamic systems with transfer functions $G_1(s)$, $G_2(s)$, $G_3(s)$ etc., occur in series, the overall transfer function, $G(s)$ can be written as [31] :-

$$G(s) = G_1(s).\, G_2(s).\, G_3(s) \qquad (2.24)$$

$$\ln G(s) = \ln G_1(s) + \ln G_2(s) + \ln G_3(s) + \ldots\ldots \qquad (2.25)$$

Thus for such a combination the moments δ, T_m, T_s^2, T_a^3 etc. are additive. This follows from equation (2.22).

$$\delta = \delta_1 + \delta_2 + \delta_3 + \ldots\ldots \qquad (2.26)$$

$$T_m = T_{m_1} + T_{m_2} + T_{m_3} + \ldots\ldots \qquad (2.27)$$

$$T_s^2 = T_{s_1}^2 + T_{s_2}^2 + T_{s_3}^2 + \ldots\ldots \qquad (2.28)$$

$$T_a^3 = T_{a_1}^3 + T_{a_2}^3 + T_{a_3}^3 + \ldots\ldots \qquad (2.29)$$

For parallel combination of the same transfer functions[33] :

$$G(s) = G_1(s) + G_2(s) + G_3(s) \ldots \qquad (2.30)$$

only the moments about the origin are additive as can be seen from equation (2.15)

$$\alpha_0 = \alpha_{01} + \alpha_{02} + \alpha_{03} \qquad (2.31)$$

$$\alpha_1 = \alpha_{11} + \alpha_{12} + \alpha_{13} \qquad (2.32)$$

$$\alpha_2 = \alpha_{21} + \alpha_{22} + \alpha_{23} \qquad (2.33)$$

$$\alpha_3 = \alpha_{31} + \alpha_{32} + \alpha_{33} \qquad (2.34)$$

The point raised in section 2.1 as to corrections which may have to be applied if the injection in the inlet stream is not exactly a dirac delta signal, can now be considered. It follows from equations (2.26 - 2.29)

that, if both the output and input distribution curves are measured, the moments of the dynamic system will be the difference between the moments calculated from these distributions.

The following relationships will also be frequently used in this work. The first set are derived from equation (2.22) :-

$$\delta = \left[\ln G(s) \right]_{s \to 0} \tag{2.35}$$

$$T_m = -\left[\frac{d \ln G(s)}{ds} \right]_{s \to 0} \tag{2.36}$$

$$T_s^2 = \left[\frac{d^2 \ln G(s)}{ds^2} \right]_{s \to 0} \tag{2.37}$$

$$T_a^3 = -\left[\frac{d^3 \ln G(s)}{ds^3} \right]_{s \to 0} \tag{2.38}$$

The remainder follow from equation (2.15) :-

$$\alpha_0 = \left[G(s) \right]_{s \to 0} \tag{2.39}$$

$$\alpha_1 = -\left[\frac{d\, G(s)}{ds} \right]_{s \to 0} \tag{2.40}$$

$$\alpha_2 = \left[\frac{d^2\, G(s)}{ds^2} \right]_{s \to 0} \tag{2.41}$$

$$\alpha_3 = -\left[\frac{d^3\, G(s)}{ds^3} \right]_{s \to 0} \tag{2.42}$$

2.23 Occurrence and Minimization of Errors in Experimental Moment Determination

It was found during the analysis of the experimental results that small errors in the measured distribution could have significant effects on the second and third moments. This was particularly so if the curves had long tails as these points would be at large time intervals away from the mean about which moments are usually taken. They are thus magnified by the $(t - T_m)^2$ and $(t - T_m)^3$ factors in equations (2.7) and (2.8) respectively. If the system contains a large proportion of "dead time" (as would be the case for long beds), the value of T_m could also be similarly affected as this moment is generally taken about the origin. It follows logically, therefore, that the above-mentioned errors would be reduced if the time axis about which moments are to be calculated is shifted towards the tail region of the curve. Denoting τ_q as the qth moment about this new axis, τ^*, and letting the error in determining E(t) be ϵ, then

$$(\tau_q)^q = \int_0^\infty (t - \tau^*)^q \, (E(t) \pm \epsilon) \, dt \qquad (2.43)$$

If t_1 is the break-away point (i.e. the point at which the E(t) curve leaves the time axis) and t_n the approximate return point (i.e. the point at which the curve becomes effectively zero). then the limits of integration in equation (2.43) can be altered such that:

$$(\tau_q)^q = \int_{t_1}^{t_n} (t - \tau^*)^q \, (E(t) \pm \epsilon) \, dt \qquad (2.44)$$

ϵ can be considered independent of t, because the main source of error in such determinations is generally the measurement of the deflection on a recorder trace, which in the case of this work could be obtained to approximately $\pm$ 0.1 mm.

$$\therefore \quad (\tau_q)^q = \int_{t_1}^{t_n} (t - \tau^*)^q \, E(t) \, dt$$

$$+ \epsilon \int_{t_1}^{\tau^*} (\tau^* - t)^q \, dt$$

$$+ \epsilon \int_{\tau^*}^{t_n} (t - \tau^*)^q \, dt \qquad (2.45)$$

(N.B. The second term in equation (2.45) has been rearranged to ensure that errors for odd moments reinforce rather than cancel each other.)

If the error in calculating $(\tau_q)^q$ is ζ_q, then

$$\zeta_q = \epsilon \int_{t_1}^{\tau^*} (\tau - t)^q \, dt$$

$$+ \epsilon \int_{\tau^*}^{t_n} (t - \tau^*)^q \, dt \qquad (2.46)$$

$$= \frac{\epsilon}{q+1} (\tau^* - t_1)^{q+1} + \frac{\epsilon}{q+1} (t_n - \tau^*)^{q+1}$$

(2.47)

$$\frac{d\zeta_q}{d\tau^*} = \epsilon\,(\tau^* - t_1)^q - \epsilon(t_n - \tau^*)^q \qquad (2.48)$$

For minimum error $\frac{d\zeta_q}{d\tau^*} = 0$

$\therefore$ For $q \neq 0$, either $\epsilon = 0$ or

$$\tau^* - t_1 = t_n - \tau^* \qquad (2.49)$$

$$\therefore \tau^* = \frac{t_n + t_1}{2} \qquad (2.50)$$

This result indicates that moments should be taken about the arithmetic mean of the break-away and return points. Once these moments have been calculated, they can be transferred to the mean via the relationships which will now be developed.

$$\tau_1 = \int_0^\infty (t - \tau^*)\, E(t)\, dt$$

$$= \int_0^\infty t\, E(t)\, dt - \tau^* \int_0^\infty E(t)\, dt$$

$$= T_m - \tau^* \qquad (2.51)$$

i.e. $$T_m = \tau^* + \tau_1 \qquad (2.52)$$

$$\tau_2^2 = \int_0^\infty \left[(t - T_m) - (\tau^* - T_m)\right]^2 E(t)\, dt$$

$$= T_s^2 + (\tau^* - T_m)^2 \qquad (2.53)$$

$$\text{i.e. } T_s^2 = \tau_2^2 + (\tau^* - T_m)^2 \qquad (2.54)$$

$$\tau_3^3 = \int_0^\infty \left[(t - T_m) - (\tau^* - T_m) \right]^3 E(t)\, dt$$

$$= T_a^3 - 3(\tau^* - T_m) T_s^2 - (\tau^* - T_m)^3 \qquad (2.55)$$

$$\text{i.e. } T_a^3 = \tau_3^3 + 3(\tau^* - T_m) T_s^2 + (\tau^* - T_m)^3 \qquad (2.56)$$

A further drawback concerning moment analysis is the estimation of t_n. Levenspiel[30] mentions this problem and suggests a value of $2T_m$. Another suggestion[24] is the fitting of a Ganssian distribution to the tail. It has been found in the present work that an exponential decay function can be adequately fitted to the tails of the curves obtained. Illustratio ns of the degree of fit are presented in Appendix 1.1.

If t_1 is the time above which the curve can be expressed as:

$$f(t) = Qe^{-Rt} \qquad (2.57)$$

then the contribution of this section of the distribution to the moments of the entire curve can be evaluated as follows:

$$f(t_1) = Qe^{-Rt_1} \qquad (2.58)$$

$$f(t) = f(t_1)\, e^{-R(t-t_1)} \qquad (2.59)$$

$$= f(t_1)\, e^{-R\tau_1} \qquad (2.60)$$

where $\tau_1 = t - t_1$

Taking moments about t_1

$$\int_{t_1}^{\infty} f(t)\,dt = f(t_1)\int_{o}^{\infty} e^{-R\tau_1}\,d\tau_1 = \frac{f(t_1)}{R} \tag{2.62}$$

$$\int_{t_1}^{\infty} (t - t_1)\,f(t)\,dt = f(t_1)\int_{o}^{\infty} \tau_1\, e^{-R\tau_1}\,d\tau_1 = \frac{f(t_1)}{R^2} \tag{2.63}$$

$$\int_{t_1}^{\infty} (t-t_1)^2\, f(t)dt = f(t_1)\int_{o}^{\infty} \tau_1^3\, e^{-R\tau_1}\,d\tau_1 = \frac{2f(t_1)}{R^3} \tag{2.64}$$

$$\int_{t_1}^{\infty} (t-t_1)^3\, f(t)dt = f(t_1)\int_{o}^{\infty} \tau_1^3\, e^{-R\tau_1}\,d\tau_1 = \frac{6\,f(t_1)}{R^4} \tag{2.65}$$

Equations (2.62 - 2.65) can then be transferred to yield their contribution of the moments about any other time axis by the method previously outlined in this section.

2.3 PREVIOUS INVESTIGATIONS

A number of methods have been employed to measure dynamic responses by the four types of disturbances mentioned in section 2.1. Injection of the tracer into the inlet stream was generally accomplished with the aid of a manually operated hypodermic syringe or an electrically operated solenoid valve which controlled the flow of tracer.

The types of tracers which have been used are radioactive materials, dyes and concentrated acid, alkali and salt solutions. The concentration measurements for the first two have usually been performed by Geiger tubes[21] and colorimetric photometers[28] respectively, whereas for the last group, titration[8] and conductivity cells[43] are favoured. Except in the case of titration, the measuring equipment produced a continuous electrical signal which was recorded on a high speed pen recorder or oscillograph.

The usual approach to the theoretical analysis of experimental results has been essentially that of solving a proposed mathematical model for the input signal used and testing for agreement with these results. If agreement was satisfactory, the characteristic model parameters were then evaluated. The three mathematical models which have found most favour among authors attempting to describe the non-ideal behaviour of liquid in a packed bed are the "Taylor diffusion model", the "Cascade of mixers model" and the "Turner model".

In the "Taylor diffusion model", the dispersion of a soluble tracer is considered to be equivalent to that of a plug flow stream with superimposed

longitudinal diffusion. The equation describing this process was first proposed by G.I. Taylor [32-34] to account for dispersion in pipe flow and was later modified by several workers[35-38]. It involves an effective axial diffusion coefficient which has been shown by Aris[39] to be equal to the sum of the molecular diffusion coefficient and a diffusion coefficient due to the velocity distribution. Experimental results for turbulent flow in straight smooth tubes[40-42] indicate that this model as modified by Tichacek et al.[38] can also be applied to this regime of flow. The procedure has since been carried a step further and the same equation has been used for packed bed flow.[23-28] The diffusion coefficient in this case is at present regarded as merely an effective parameter which has to be experimentally determined.

The "cascade of mixers model"[23] postulates that the deviation from plug flow results from a number of completely mixed cells connected in series. As in the case of the previous model, the characteristic parameter, i.e. number of mixers, has not as yet been related theoretically to the physical set up.

The "Turner Model" was first proposed by G.A. Turner[44] to account for diffusion into stagnant pockets in single phase packed bed flow. The treatment was extended by Glaser and Litt[45], who derived the first and second moments of the model in terms of three shape factors, which are functions of the packing alone. Their analyses applies only to laminar flow, but could be extended to the general case with the introduction of further parameters. It is probable that this model is basically closer to the actual system than the former two with the result that the parameters of such a model will have far more physical significance. It has the disadvantage, however, of containing a larger number of parameters and would prove more difficult to manipulate mathe-

matically when applied to the study of reaction kinetics and mass transfer.

The majority of experimental data for packed beds has been for single phase flow[23,26,27,28,43] Mixing of the liquid stream in two phase gas-liquid flow with Raschig ring packings was studied by Otake and Kunugita[46], who correlated their results by the equation:

$$\frac{D\rho}{\mu} = 0.527 \left(\frac{d_p \bar{u} \rho}{\mu} \right)^{1/2} \left(\frac{d_p^3 \rho^2 g}{\mu^2} \right)^{1/3} \qquad (2.66)$$

where D is the effective axial diffusion coefficient. The results of King[8], who used 0.6 cm. Raschig rings agreed fairly well with this correlation.

Glaser and Litt[45] obtained residence time distribution data for a 1" I.D. column packed with 10 to 14 mesh particles at low liquid rates. Their results could be correlated by the equation:

$$\gamma_1^2 = \frac{T_s^2}{T_m^2} = A_0 + A_1 \left(\frac{d_p \bar{u} \rho}{\mu} \right) \qquad (2.67)$$

where A_0 and A_1 are functions of the bed geometry and physical properties of the liquid. Equation (2.67) is a verification of the "Turner model" in the laminar flow regime[45].

2.4 THEORETICAL ANALYSIS

2.41 Models to be used in the present study.

Two models have been selected for the present work. The first, to be labelled "Model A" is basically the same as the "Taylor Diffusion Model", however, allowance is to be made for a possible variation in the mean longitudinal velocity and effective axial diffusion coefficient according to radial position in the bed. The "Taylor Diffusion Model" is chosen to describe the flow conditions in a particular channel in the packing because of its close degree of fit to systems of a similar nature, e.g. pipe-flow[32] and film flow[50]. The modifications which are to be imposed will enable an assessment to be made of the effects of non-uniform liquid distribution.

The model postulates that the liquid flows down a number of preferential channels in the bed. If these are numbered from 1 to n, then for the rth stream the concentration of the tracer at distance x from the top of the bed and time t from the injection of a pulse is $C_r(x,t)$. If the liquid flows with mean linear velocity $\bar{u}_r$ and has a longitudinal coefficient of dispersion D_r, then a mass balance over a small increment of this channel results in the equation[32]

$$D_r \frac{\partial^2 C_r(x,t)}{\partial x^2} - \bar{u}_r \frac{\partial C_r(x,t)}{\partial x} = \frac{\partial C_r(x,t)}{\partial t} \qquad (2.68)$$

The boundary conditions for this equation are:-

(a) For a unit dirac delta function at $x = 0$;

$$C_r(0,t) = 1 \qquad (2.69)$$

(b) When $t = 0$, the concentration is zero at all

$$x > 0$$

i.e. $$C_r(x,0) = 0 \qquad (2.70)$$

(c) The third boundary condition for the diffusion equation has been the subject of much discussion in the literature[47] . The one favoured by most authors is the condition of negligible longitudinal dispersion at large stream lengths, i.e.

$$\lim_{x \to \infty} \frac{\partial C_r(x,t)}{\partial x} = 0 \qquad (2.71)$$

The second model "Model B", is to be introduced in an attempt to estimate the mass transfer coefficient by means of a purely hydrodynamic technique, such as the pulse testing, employed in this work. The model considers each of the streams as a thin film in laminar flow. Due to the discontinuous nature of the packing, it is postulated that a certain amount of lateral mixing occurs to varying degrees as the liquid passes down a channel in the bed. The derivation and solution of the equation describing the dispension of soluble matter in this system would be too complicated to handle as such. Instead the approach can be simplified by saying that the actual conditions postulated can be fitted to a model where complete lateral mixing of the film occurs at equal intervals down the bed. The form of the model is similar to that of Higbie[2] for gas absorption in a packed column. This is the so-called "Penetration Model" which assumes that the bulk of the liquid stream mixes with the interfacial layers at fixed intervals down the bed, thus exposing fresh surface to the gas at these points. The steady-state diffusion equation for the absorption of a gas in the laminar film between each mixing section has been solved for a number of processes[2] . For the purposes of this analysis the transient equation for the dispersion of

tracer in this film is required. As the shape of the velocity profile will have a profound effect on the solution, one of the aims of Model B is to describe the development of this profile from a uniform value at the mixing points to one which tends to a parabolic form lower down the film.

Figure 1 gives a diagrammatic picture of a section of the rth channel. Considering the region between any two mixing points, the equation describing the concentration $C_r(x, y, t)$ of a soluble material in the film is:

$$\frac{\partial C_r(x, y, t)}{\partial t} = - u_r(x, y) \frac{\partial C_r(x, y, t)}{\partial x} \qquad (2.72)$$

This assumes that all terms, apart from the longitudinal convection term, are negligible. Boundary conditions for this equation are:

(a) When $t = 0$, $C_r(x, y, o) = 0$ (2.73)

(b) For a unit dirac delta input at $x = 0$;

$$C_r(0, y, s) = 1 \qquad (2.74)$$

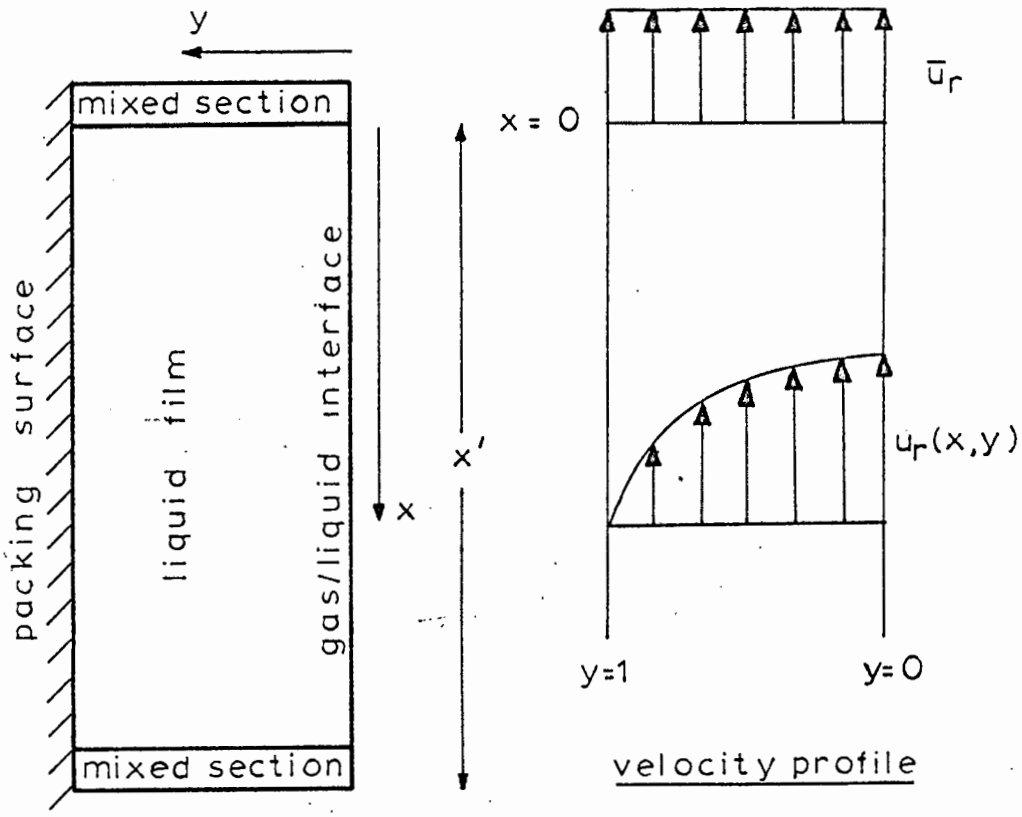
y
mixed section
packing surface
liquid film
gas/liquid interface
x
x'
mixed section
x = 0
$\bar{u}_r$
$u_r(x,y)$
y=1
y=0
velocity profile

FIGURE 1

2.42 Derivation of moments for Model A.

Transforming equation (2.68) by La Place with respect to x and t, denoting P and s as the transforms of x and t respectively,

$$D_r\left[P^2 C_r(P,s) - PC_r(O,s) - C_r'(O,s)\right] - \bar{u}_r\left[P C_r(P,s) - C_r(O,s)\right]$$

$$= s\, C_r(P,s) - C_r(x,o) \qquad (2.75)$$

where $C_r'(O,s) = \lim_{x \to o} \frac{\partial C_r(x,s)}{\partial x}$ (2.76)

Substituting equations (2.69) and (2.70) in (2.75)

$$C_r(P,s)\left[P^2 - \frac{\bar{u}_r}{D_r} - \frac{s}{D_r}\right] = P - \frac{\bar{u}_r}{D_r} + C_r'(o,s) \qquad (2.77)$$

$$C_r(P,s) = \frac{P + \beta_o}{(P + \beta_1)(P + \beta_2)} \qquad (2.78)$$

where $\beta_o = -\frac{\bar{u}_r}{D_r} + C_r'(o,s)$ (2.79)

$$\beta_1 = -\frac{\bar{u}_r}{2D_r} + \sqrt{\frac{\bar{u}_r^2}{4D_r^2} + \frac{s}{D_r}} \qquad (2.80)$$

$$\beta_2 = -\frac{\bar{u}_r}{2D_r} - \sqrt{\frac{\bar{u}_r^2}{4D_r^2} + \frac{s}{D_r}} \qquad (2.81)$$

Inverse transforming (2.78) with respect to P

$$C_r(x,s) = \frac{(\beta_0-\beta_1)^{-\beta_1 x} - (\beta_0-\beta_2)^{-\beta_2 x}}{\beta_2-\beta_1} \qquad (2.82)$$

$$\therefore \frac{\partial C_r(x,s)}{\partial x} = \frac{-\beta_1(\beta_0-\beta_1)}{(\beta_2-\beta_1)} e^{-\beta_1 x} + \frac{\beta_2(\beta_0-\beta_2)}{\beta_2-\beta_1} e^{-\beta_2 x}$$

Using equation (2.71),

$$\lim_{x\to\infty} \frac{\partial C_r(x,s)}{\partial x} = \lim_{x\to\infty} \left[\frac{-\beta_1(\beta_0-\beta_1)}{\beta_2-\beta_1} e^{-\beta_1 x} + \frac{\beta_2(\beta_0-\beta_2)}{\beta_2-\beta_1} e^{-\beta_2 x} \right]$$

$$= 0 \qquad (2.84)$$

Now, $\lim_{x\to\infty} e^{-\beta_1 x} = 0 \qquad (2.85)$

but $\lim_{x\to\infty} e^{-\beta_2 x} \neq 0 \qquad (2.86)$

$\therefore \beta_0 = \beta_2 \qquad (2.87)$

Substituting (2.87) in (2.82)

$$C_r(x,s) = e^{-\beta_1 x} \qquad (2.88)$$

If the concentration of tracer in the stream is measured at distance L from the top of the bed,

$$C_r(L,s) = \exp\left[\frac{\bar{u}_r L}{2D_r} - \sqrt{\frac{\bar{u}_r^2 L^2}{4D_r} + \frac{sL^2}{D_r}} \right] \qquad (2.89)$$

Applying equations (2.35), 2.36), 2.37 and (2.38):

$$\delta_r = 0 \tag{2.90}$$

$$T_{mr} = \frac{L}{\bar{v}_r} \tag{2.91}$$

$$T_{sr}^2 = \frac{2L\,D_r}{\bar{v}_r^3} \tag{2.92}$$

$$T_{ar}^3 = \frac{12\,L\,D_r^2}{\bar{v}_r^5} \tag{2.93}$$

If the quantity ϕ is defined by the equation:

$$\phi = \frac{T_m\,T_a^3}{T_s^4} \tag{2.94}$$

then for any stream of Model A,

$$\phi = \frac{T_{mr}\,T_{ar}^3}{T_{sr}^4} = 3 \tag{2.95}$$

2.43 Derivation of Moments for Model B.

Transforming equation (2.72) with respect to t:

$$s\,C_r(x,y,s) - C_r(x,y,o) = -u_r(x,y)\frac{\partial C_r(x,y,s)}{\partial x} \qquad (2.96)$$

Substituting boundary condition (a)

$$\frac{\partial C_r(x,y,s)}{C_r(x,y,s)} = \frac{-s\,\partial x}{u_r(x,y)} \qquad (2.97)$$

$$\int_{C_r(o,y,s)}^{C_r(x',y,s)} \frac{C_r(x,y,s)}{C_r(x,y,s)} = -\int_o^{x'} \frac{s\,\partial x}{u_r(x,y)} \qquad (2.98)$$

Using boundary condition (b)

$$C_r(x',y,s) = \exp\left[-s\int_o^{x'} \frac{\partial x}{u_r(x,y)}\right]$$

$$= e^{-sW_r(x',y)} \qquad (2.99)$$

where $$W_r(x',y) = \int_o^{x'} \frac{\partial x}{u_r(x,y)} \qquad (2.100)$$

If at x' the film is suddenly mixed to give a uniform concentration $C_r(x',t)$, then by material balance at this point:

$$C_r(x',t) = \int_o^1 \frac{u_r(x'y)}{\bar{u}_r} C_r(x,'y,t)\,dy \qquad (2.101)$$

Transforming with respect to t,

$$C_r(x',s) = \int_0^1 \frac{\bar{u}_r(x',y)}{\bar{u}_r} C_r(x',y,s)\, dy \qquad (2.102)$$

$$= \int_0^1 \frac{u_r(x',y)}{\bar{u}_r} e^{-sW_r(x',y)}\, dy \qquad (2.103)$$

Expanding the exponential term,

$$C_r(x',s) = \int_0^1 \frac{u_r(x',y)}{\bar{u}_r} dy - s\int_0^1 \frac{u_r(x',y)}{\bar{u}_r} W_r(x,'y)\, dy + \tfrac{1}{2} s^2 \int_0^1 \frac{u_r(x',y)}{\bar{u}_r} \left[W_r(x,'y)\right]^2 dy$$

..... (2.104)

The mean velocity $\bar{u}_r = \int_0^1 u_r(x',y)\, dy \qquad (2.105)$

$$\therefore \alpha_0' = \int_0^1 \frac{u_r(x',y)}{\bar{u}_r} dy = 1 \qquad (2.106)$$

$$\alpha_1' = \int_0^1 \frac{u_r(x',y)}{\bar{u}_r} W_r(x',y)\, dy \qquad (2.107)$$

$$\alpha_2' = \int_0^1 \frac{u_r(x',y)}{\bar{u}_r} W_r(x',y)\, dy \qquad (2.108)$$

$$\alpha_3' = \int_0^1 \frac{u_r(x',y)}{\bar{u}_r} \left[W_r(x',y)\right]^3 dy \qquad (2.109)$$

From the relationships derived in Section 2.22

$$T_m' = \alpha_1' \tag{2.110}$$

$$(T_s') = \alpha_2' - (\alpha_1')^2 \tag{2.111}$$

$$(T_a')^3 = \alpha_3' - 3\alpha_2'\alpha_1' + 2(\alpha_1')^3 \tag{2.112}$$

If the total number of mixing stages in a bed length L is q,

i.e.
$$L = qx' \tag{2.113}$$

$$T_{mr} = q\,T_m' \tag{2.114}$$

$$T_{sr}^2 = q\,(T_s')^2 \tag{2.115}$$

$$T_{ar}^3 = q\,(T_a')^3 \tag{2.116}$$

The above relationships result from the fact that the individual regions making up the total stream occur in series.

To determine T_{mr}, T_{sr}^2 and T_{ar}^3, the integrals in equations (2.107), (2.108) and (2.109) will have to be evaluated. This requires the velocity profile to be known as a function of x and y. Wang and Longwell[48] have calculated theoretical velocity profiles at the entrance region of two parallel plates placed in a fluid moving with uniform velocity. Their analysis involved the numerical solution of the momentum equations. The profile for a laminar film will be expected to be the same as that for flow between parallel plates from the surface of one to the centre plane. The latter will correspond

to the interface. It is proposed for the purpose of this work to fit a simple algebraic equation to their results. The equation chosen is:

$$\frac{u_r(x,y)}{\bar{u}_r} = \frac{1}{1 - HZ} \tag{2.117}$$

where $$H = 1 - \frac{2}{3(1 - y^2)} \tag{2.118}$$

$$Z = 1 - \frac{1}{1 + mx} \tag{2.119}$$

and m is a constant.

In Appendix 1:2 the velocity profiles obtained from equation (2.117) are compared with those of Wang and Longwell as well as those of Schlichting as reported by them.[48]

Using equation (2.117)

$$W_r(x',y) = \int_0^{z'} \frac{(1 - HZ)\ \partial Z}{\ln \bar{u}_r (1 - Z)^2} \tag{2.120}$$

where $$Z' = 1 - \frac{1}{1 + mx'} \tag{2.121}$$

Integrating:

$$W_r(x',y) = \frac{x'}{\bar{u}_r} \left(\frac{1 - Z'}{Z'}\right)\left[\frac{1 - HZ'}{1 - Z'} - H \ln (1 - Z') - 1\right] \tag{2.122}$$

$$T_m' = B_1 \frac{x'}{\bar{u}_r} \left(\frac{1 - Z'}{Z'}\right) \tag{2.123}$$

$$(T_s')^2 = B_2 \left(\frac{x'}{\bar{u}_r}\right)^2 \left(\frac{1 - Z'}{Z'}\right)^2 \tag{2.124}$$

$$(T_a')^3 = B_3 \left(\frac{x'}{\bar{u}_r}\right)^3 \left(\frac{1 - Z'}{Z'}\right)^3 \tag{2.125}$$

where $$B_1 = \int_0^1 \frac{1}{1 - HZ'} \left[\frac{1 - HZ'}{1 - Z'} - H \ln (1 - Z') - 1\right]^2 dy \tag{2.126}$$

$$B_2 = \int_0^1 \frac{1}{1 - HZ'} \left[\frac{1 - HZ'}{1 - Z'} - H \ln (1 - Z') - 1\right]^2 dy \tag{2.127}$$

$$B_3 = \int_0^1 \frac{1}{1 - HZ'} \left[\frac{1 - HZ'}{1 - Z'} - H \ln (1 - Z') - 1\right]^3 dy \tag{2.128}$$

$$T_{mr} = qB_1 \frac{x'}{\bar{u}_r} \left(\frac{1 - Z'}{Z'}\right) = B_1 \frac{L}{\bar{u}_r} \left(\frac{1 - Z'}{Z'}\right) \tag{2.129}$$

$$T_{sr}^2 = B_2 \frac{x'L}{\bar{u}_r^2} \left(\frac{1 - Z'}{Z'}\right)^2 \tag{2.130}$$

$$T_{ar}^3 = B_3 \frac{(x')^2 L}{\bar{u}_r^3} \left(\frac{1 - Z'}{Z'}\right)^3 \tag{2.131}$$

$$\phi = \frac{T_{mr} T_{ar}^3}{T_{sr}^4} = \frac{B_1 B_3}{B_2^2} \tag{2.132}$$

2.44 Moments of a single outlet stream which has been formed by combining a number of parallel streams.

The moments of parallel stream models have been discussed by the author in a recent paper[61]. The following is the application of principles which were introduced to the case of n parallel channels in a packed bed.

If C_r (L,t) is the concentration of tracer in the r th channel at the base of a packed height L, Ar the fraction of the total flow of liquid passing down this channel and $Co(L,t)$ the outlet concentration from the column when all streams are combined,

$$C_o(L,t) = \sum_{r=1}^{n} A_r C_r (L,t) \qquad (2.133)$$

Transforming with respect to t,

$$C_o(L,s) = \sum_{r=1}^{n} A_r C_r(L,s) \qquad (2.134)$$

Comparing this with equation (2.30) and using the relationships derived in Section 2.22,

$$\alpha_0 = \Sigma\ A_r\ \alpha_{0r} \qquad (2.135)$$

$$\alpha_1 = \Sigma\ A_r\ \alpha_{1r} \qquad (2.136)$$

$$\alpha_2 = \Sigma\ A_r\ \alpha_{2r} \qquad (2.137)$$

$$\alpha_3 = \Sigma\ A_r\ \alpha_{3r} \qquad (2.138)$$

Now for each stream,

$$\alpha_{0r} = 1 \text{ (normalised distribution)} \quad (2.139)$$

$$\alpha_{1r} = T_{mr} \quad (2.140)$$

$$\alpha_{2r} = T_{sr}^2 - T_{mr}^2 \quad (2.141)$$

$$\alpha_{3r} = T_{ar}^3 + 3T_{sr}^2 T_{mr} + T_{mr}^3 \quad (2.142)$$

Therefore:

$$T_m = \frac{\alpha_1}{\alpha_0} = a_1 L \quad (2.143)$$

$$T_s^2 = \frac{\alpha_2}{\alpha_0} - \left(\frac{\alpha_1}{\alpha_0}\right)^2 = b_1 L + b_2 L^2 \quad (2.144)$$

$$T_a = \frac{\alpha_3}{\alpha_0} - \frac{3\alpha_2\alpha_1}{\alpha_0^2} + 2\left(\frac{\alpha_1}{\alpha_0}\right)^3$$

$$= C_1 L + C_2 L^2 + C_3 L^3 \quad (2.145)$$

where

$$a_1 = \Sigma A_r T_{mr} / L \quad (2.146)$$

$$b_1 = \Sigma A_r T_{sr}^2 / L \quad (2.147)$$

$$b_2 = \Sigma A_r T_{mr}^2 / L^2 - (\Sigma A_r T_{mr} / L)^2 \quad (2.148)$$

$$c_1 = \Sigma A_r T_{ar}^3 / L \quad (2.149)$$

$$c_2 = 3\Sigma A_r T_{mr} T_{sr}^2 / L^2 - 3\Sigma A_r T_{mr} / L \; \Sigma A_r T_{sr}^2 / L^2 \quad (2.150)$$

$$c_3 = \Sigma A_r T_{mr}^3 / L^3 - 3\Sigma A_r T_{mr}^2 / L^2 \; \Sigma A_r T_{mr} / L + 2(\Sigma A_r T_{mr} / L)^3 \quad (2.151)$$

As T_{mr}, T_{sr}^2 and T_{ar}^3 are proportional to L for both Model A and B, the parameters a_1, b_1, b_2, c_1, c_2 and c_3 are independent of bed height. (Note: whenever the symbol Σ has been used in this subsection it refers to $\sum_{r=1}^{n}$).

2.5 APPARATUS AND EXPERIMENTAL PROCEDURE

The basic apparatus consisted of a 3" I.D. glass column which could be packed to depths up to 9 ft. The packing used in all runs was $\frac{1}{4}$" porcelain Berl saddles. A schematic diagram of the column arrangement is shown in Fig.2(a). The input and output signals were measured by means of conductivity cells which are also shown in this diagram. The cells were each connected to two similar recording systems, one of which is shown diagrammatically in Fig. 2(b). For the radial residence time distribution measurements the base of the tower was modified as illustrated in Fig. 2(c).

The water rotameter was calibrated by weighing the effluent from the column over a given period of time. The curve of water rate versus rotameter scale reading is presented in Fig.3.

Calibration of the concentration measuring system involved the preparation of a set of standard NaOH solutions. The outlet from the conductivity cell was closed and the cell filled with each solution in turn. The recorder was zeroed by adjusting the balancing potentiometer in the Wheatstone Bridge when water alone filled the cell. Without altering the electrical set up, the deflection on the recorder was read for various alkaline concentrations. The results are plotted in Fig.4. It can be seen that the response of the measuring system is linear, with the result that the recorder deflections can be used directly to obtain the E (t) curves.

Before commencing a series of runs at a given packed height, the liquid was allowed to flow for 5 to 10 minutes at a rate considerably higher than the value to be used. After adjusting to the required flow rate, a further

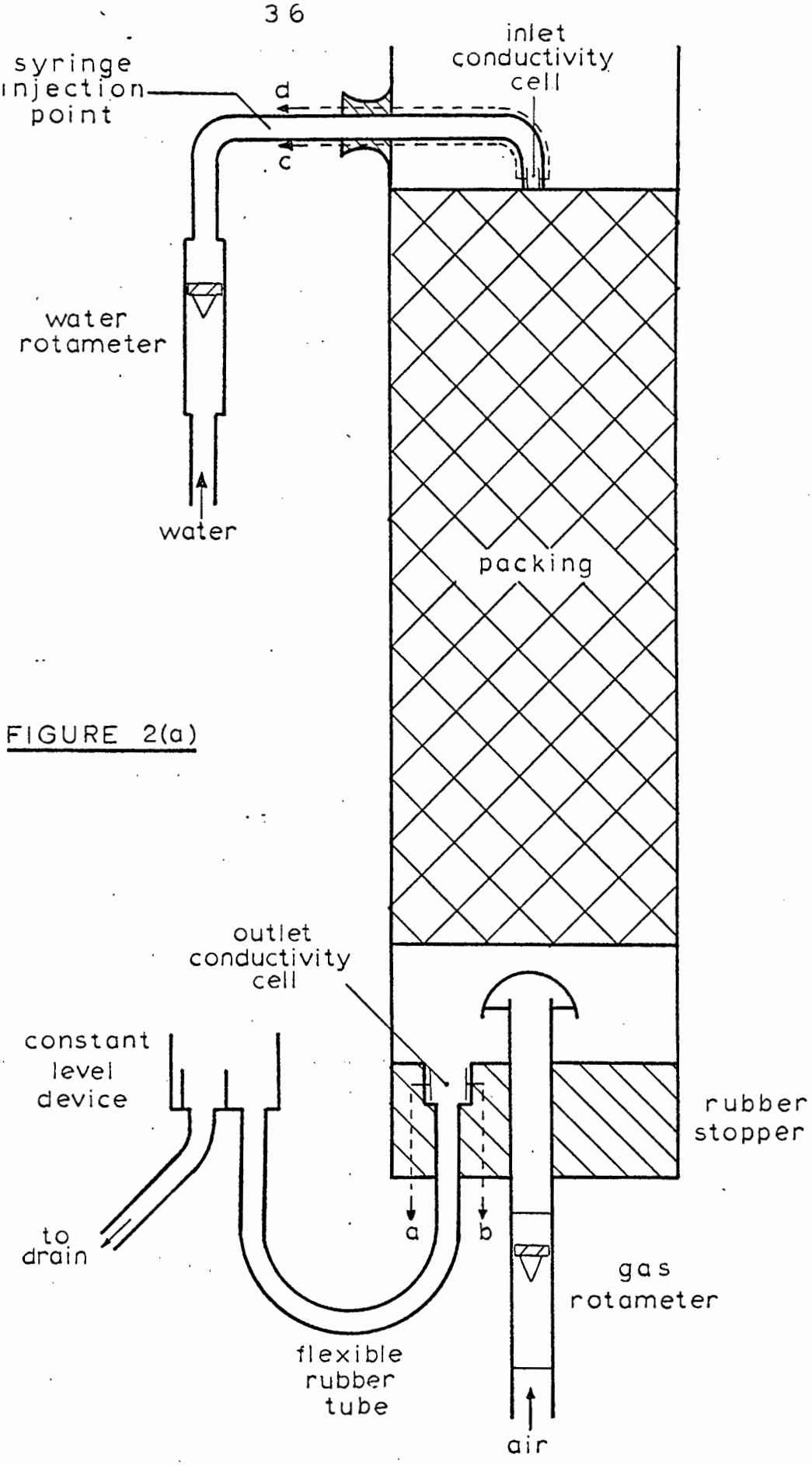
syringe injection point
d
c
inlet conductivity cell
water rotameter
water
packing
outlet conductivity cell
constant level device
to drain
a
b
rubber stopper
gas rotameter
flexible rubber tube
air

FIGURE 2(a)

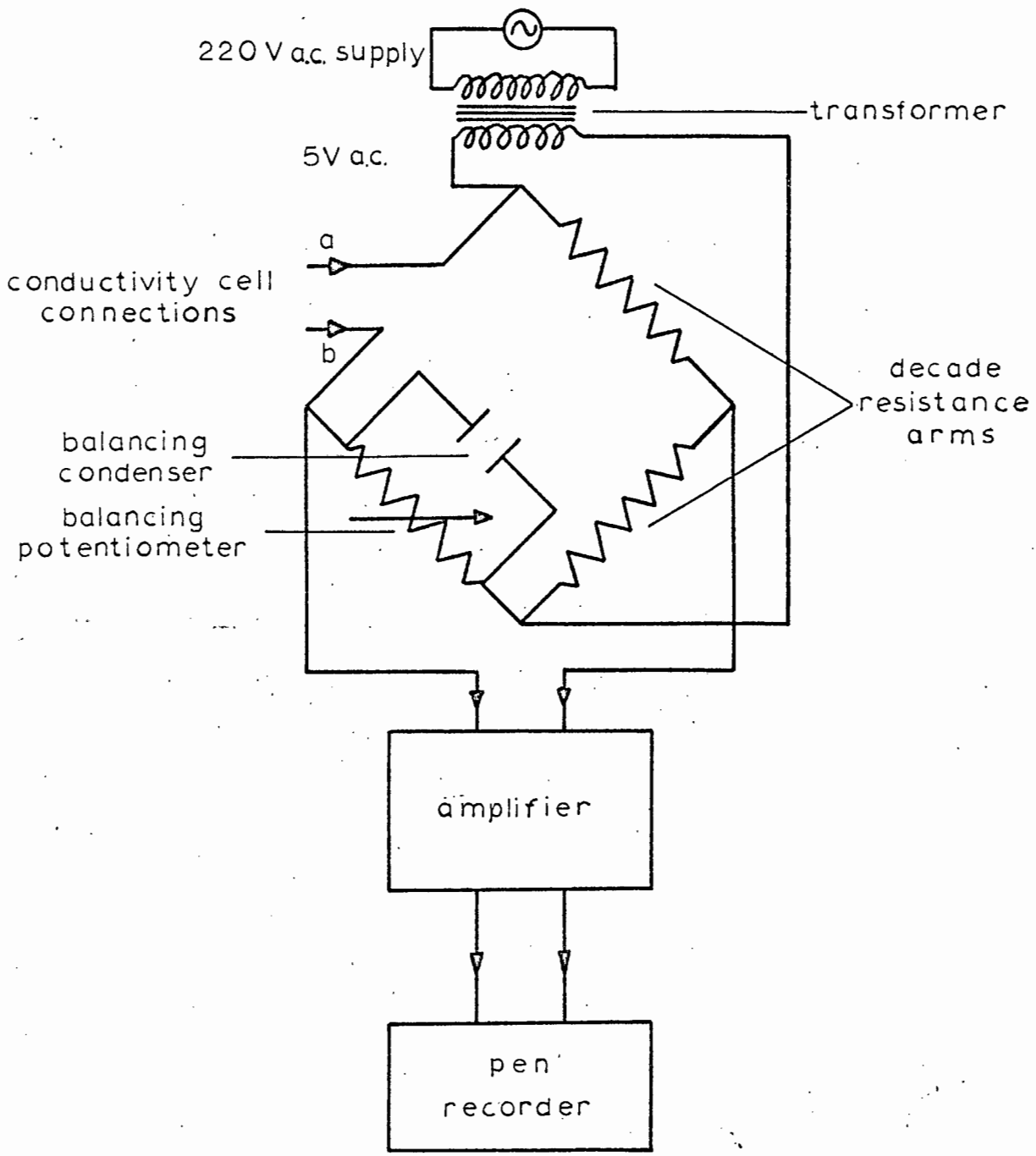
220 V a.c. supply
transformer
5V a.c.
a
conductivity cell
connections
b
decade
resistance
arms
balancing
condenser
balancing
potentiometer
amplifier
pen
recorder

FIGURE 2(b)

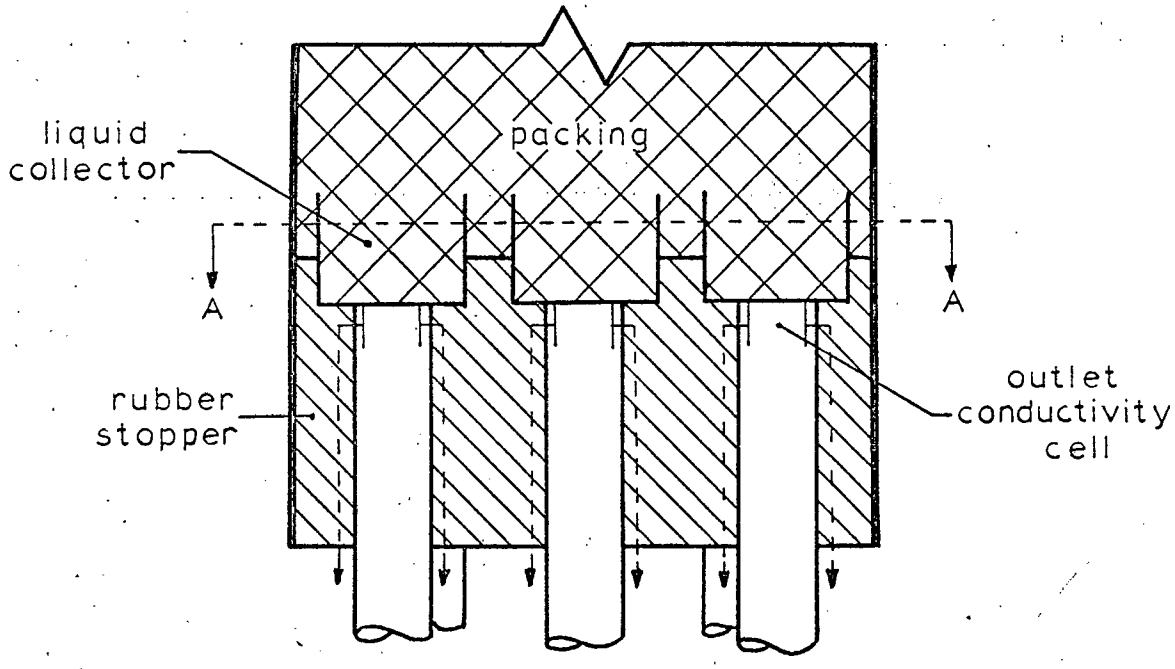

SIDE VIEW IN SECTION

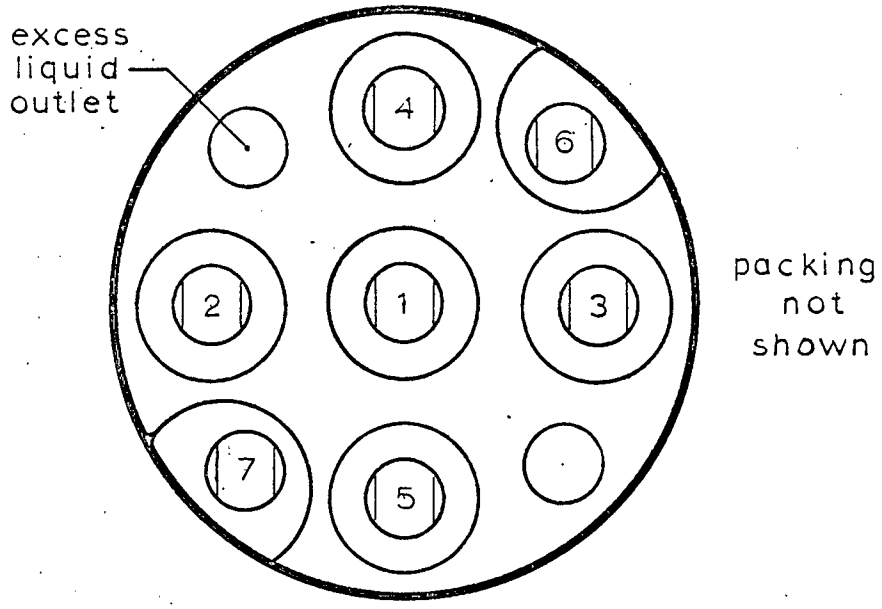

SECTION AA

FIGURE 2(c)

Scale: Full Size

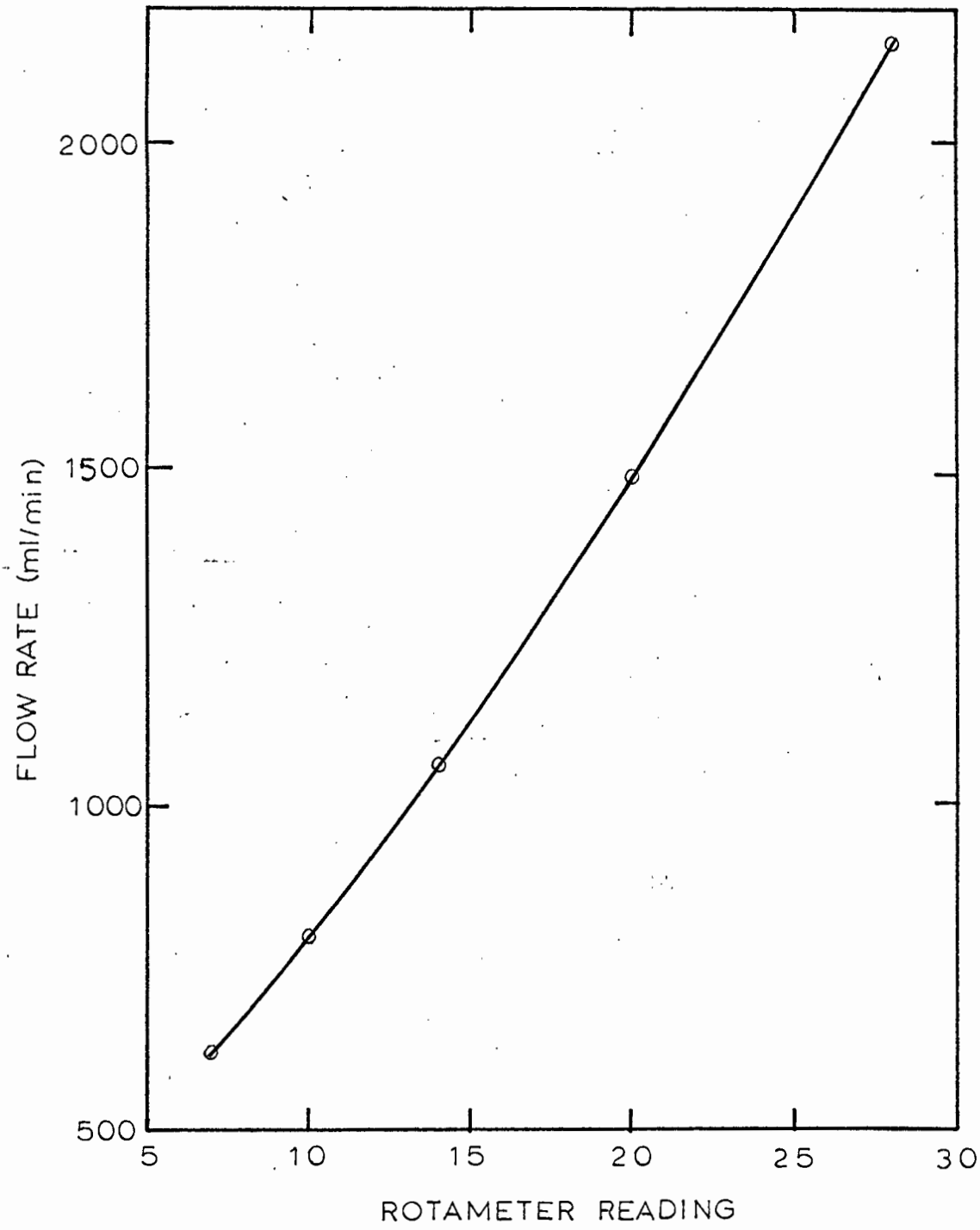
2000
1500
1000
500
FLOW RATE (ml/min)
5
10
15
20
25
30
ROTAMETER READING

FIGURE 3

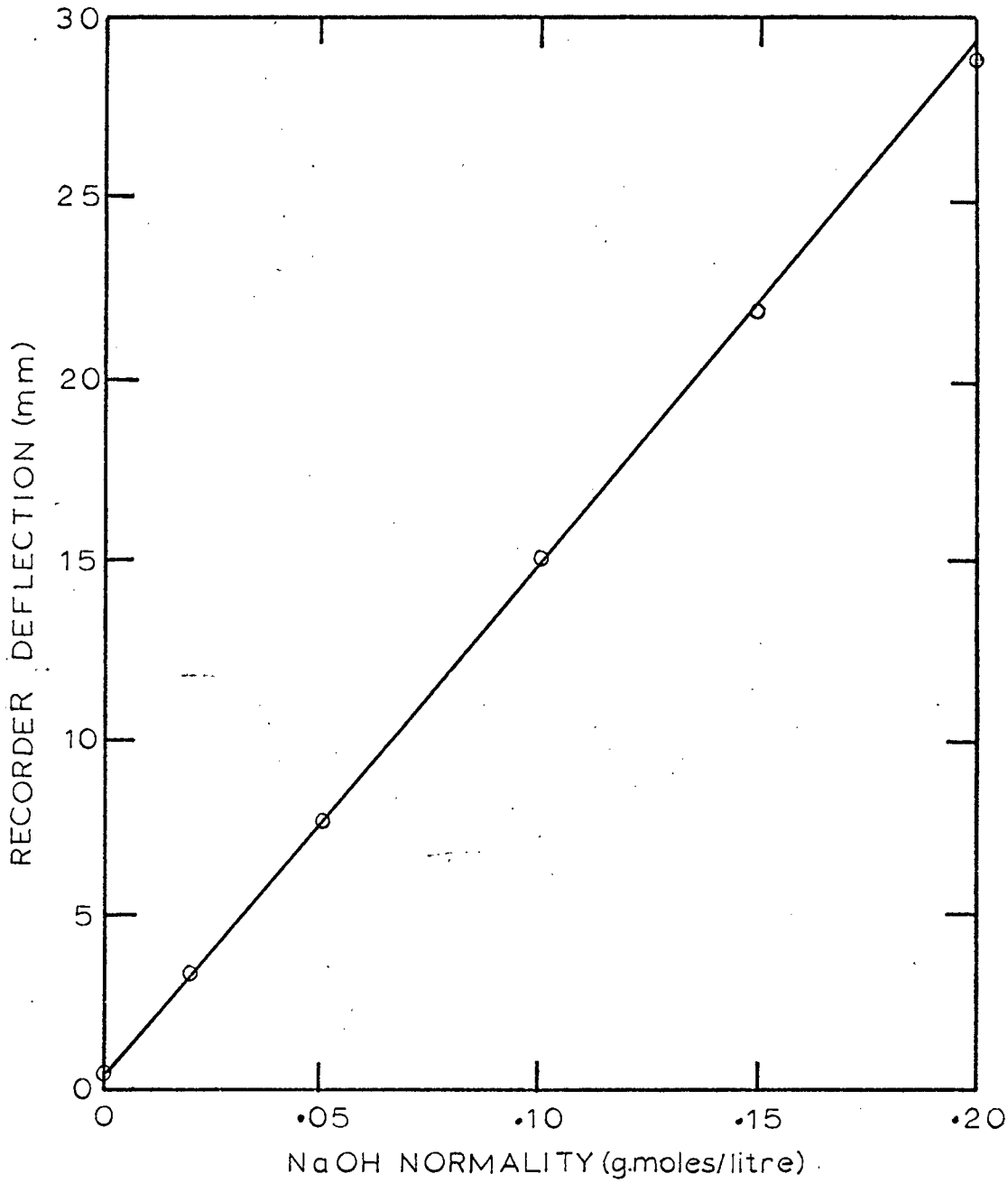
30
25
20
15
10
5
0
RECORDER DEFLECTION (mm)
0
·05
·10
·15
·20
NaOH NORMALITY (g.moles/litre)

FIGURE 4

10 minutes was allowed before a pulse of concentrated NaOH was injected with a hyperdermic syringe. The measurement of the output curve was terminated when the reading on the recorder was less than about 0.3 mm. A series of such runs was performed at four flow rates, each at four different packed heights with a constant air-rate of 40 litres/min. The above procedure was twice repeated so that a total of three results was obtained for each height and flow rate used.

For the radial measurements, the injection of the pulse was performed seven times under steady flow conditions. Prior to the injection, the output recorder was connected in turn to each of the cells at the base of the tower and the recorder set to zero deflection. On completion of the seven residence time distribution curves, the flow rate from each cell was measured. This was done by collecting liquid samples from the outlet of the individual cells over a given period of time and determining their volumes with the aid of a measuring cylinder.

2.6 RESULTS

Typical input and output curves as read from the recorder chart are shown in Figs. 5(a) and 5 (b) respectively. Smooth curves could generally be drawn through the data obtained from the recorder trace with the exception of a few runs at low packed heights. These showed very small, almost periodic fluctuations superimposed on the general trends of the output curves particularly in the regions before the peaks. It is postulated that these are due to small variations in the liquid flow rate caused by a dripping action from one packing piece to another. The phenomenon was clearly visible at a number of points on the column wall when the tower was in operation. As the concentration-time curves are steepest in the regions just before the peaks, variations of this nature would be expected to have most effect here. For the purposes of analysing the results by determining moments, smoothed values were used in these regions.

The choice of moment characterisation and the definitions of the parameters involved have been discussed in Section 2.21. The first, second and third moments have been determined for the input and output tracer distribution curves for all the runs performed. As moments are additive for transfer functions in series, the moments of the system can be obtained by sub tracting input moments from the corresponding output moments. Calculations were performed on an I.C.T. 1301 digital computer, the program for which is discussed in Appendix 2.1.

A preliminary set of results was performed to investigate the effect of air rate on the moments of the liquid side residence time distribution curve. The values for a packed height of 114 cms. and a water rate of 33.6 ml/sec. are tabulated below:

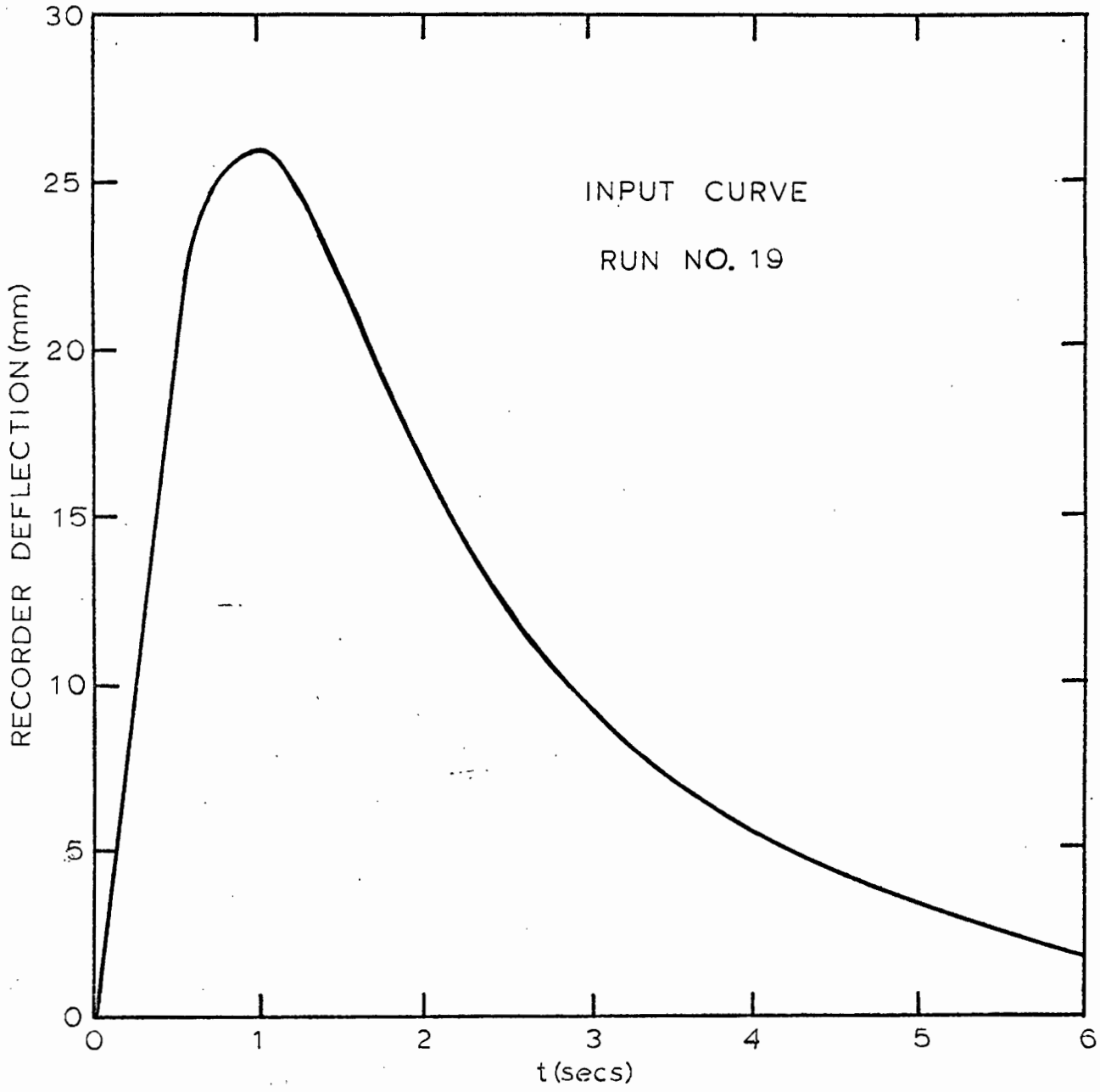
INPUT CURVE
RUN NO. 19
RECORDER DEFLECTION (mm)
t (secs)
0
5
10
15
20
25
30
0
1
2
3
4
5
6

FIGURE 5(a)

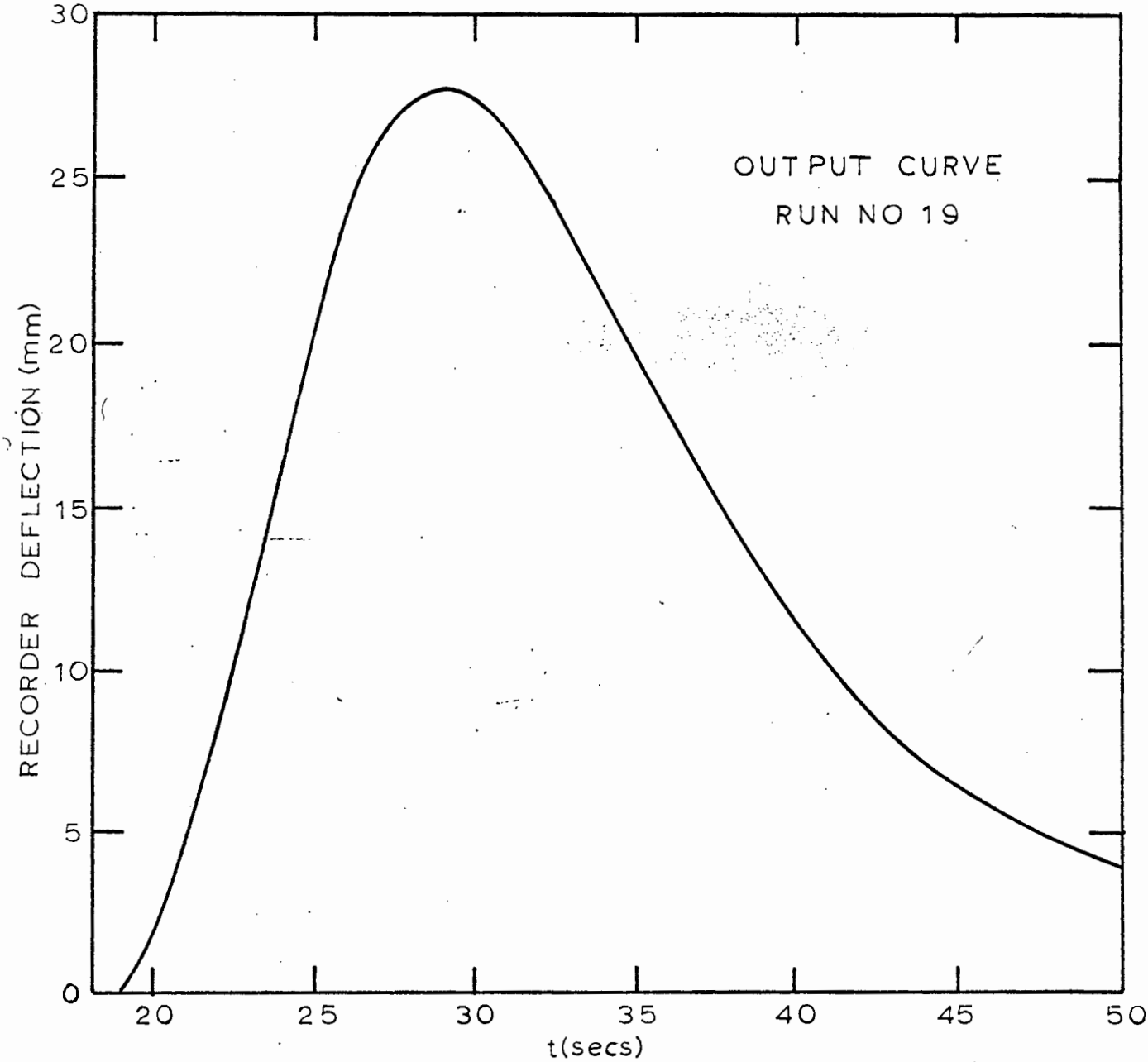
OUTPUT CURVE
RUN NO 19
RECORDER DEFLECTION (mm)
0
5
10
15
20
25
30
20
25
30
35
40
45
50
t(secs)

FIGURE 5(b)

TABLE 1.

AIR RATE (litres/min.)	T_m (secs.)	T_s^2 (sec.^{2})	T_a^3 (sec.^{3})
0	33.0	40.8	234
20	32.8	42.3	257
40	34.1	41.2	223

These results indicate that the air rate has no apparent effect in the range of flow rates used. All subsequent runs were performed with an air rate of 40 litres/min. with the exception of the series of seven point radial measurements where no gas rate was used. This was due to the fact that the sampling system at the base of the tower for these runs left insufficient space to accommodate a gas inlet arrangement.

The results for the column with single outlet are presented in Table 2. The first set are numbered from 1 to 16, the second from 17 to 32 and the third from 33 to 48. In Appendix 1.3, the values of the moments for input and output signals are recorded.

TABLE 2.

RUN No.	WATER RATE (ml./sec.)	PACKED HEIGHT (cms.)	T_m (secs.)	T_s^2 (sec.^{2})	T_a^3 (sec.^{3})
1	15.4	114	54.3	157	2110
2		84	39.7	109	1380
3		69	32.3	88	1130
4		38	16.9	52	690

5	20.2	114	45.4	98	1061
6		84	32.8	64.6	535
7		69	26.6	50.7	422
8		38	14.6	29.2	236
9	26.2	114	37.5	58.2	368
10		84	27.3	39.9	209
11		69	22.3	32.8	168
12		38	12.6	18.0	89
13	33.6	114	32.6	43.0	193
14		84	23.1	29.4	123
15		69	19.0	23.4	100
16		38	10.0	13.0	56
17	15.4	114	54.3	166	2766
18		84	39.9	112	1641
19		69	32.2	88.5	1416
20		38	17.0	47.4	688
21	20.2	114	45.9	103	1421
22		84	33.0	66.8	666
23		69	27.0	52.4	580
24		38	14.5	27.7	284
25	26.2	114	38.5	65.5	664
26		84	27.7	44.1	300
27		69	23.1	36.4	284
28		38	12.2	19.1	129

29	33.6	114	34.3	39.3	263
30		84	23.5	29.5	191
31		69	19.4	24.0	120
32		38	10.3	12.7	54.8
33	15.4	114	54.9	176	2870
34		84	40.6	120	1891
35		69	32.5	98	1688
36		38	17.4	51.9	721
37	20.2	114	46.8	90.6	952
38		84	33.3	69.7	697
39		69	27.9	54.2	611
40		38	15.1	28.9	300
41	26.2	114	39.1	75.3	763
42		84	28.1	45.4	334
43		69	23.6	39.4	302
44		38	12.6	21.4	139
45	33.6	114	34.5	40.4	287
46		84	24.1	33.2	206
47		69	20.1	25.3	157
48		38	10.4	13.2	62.3

These values are plotted in Figs. 6(a), 6 (b) and 6(c). The solid lines represent the best linear fit for each flow rate and are described by the

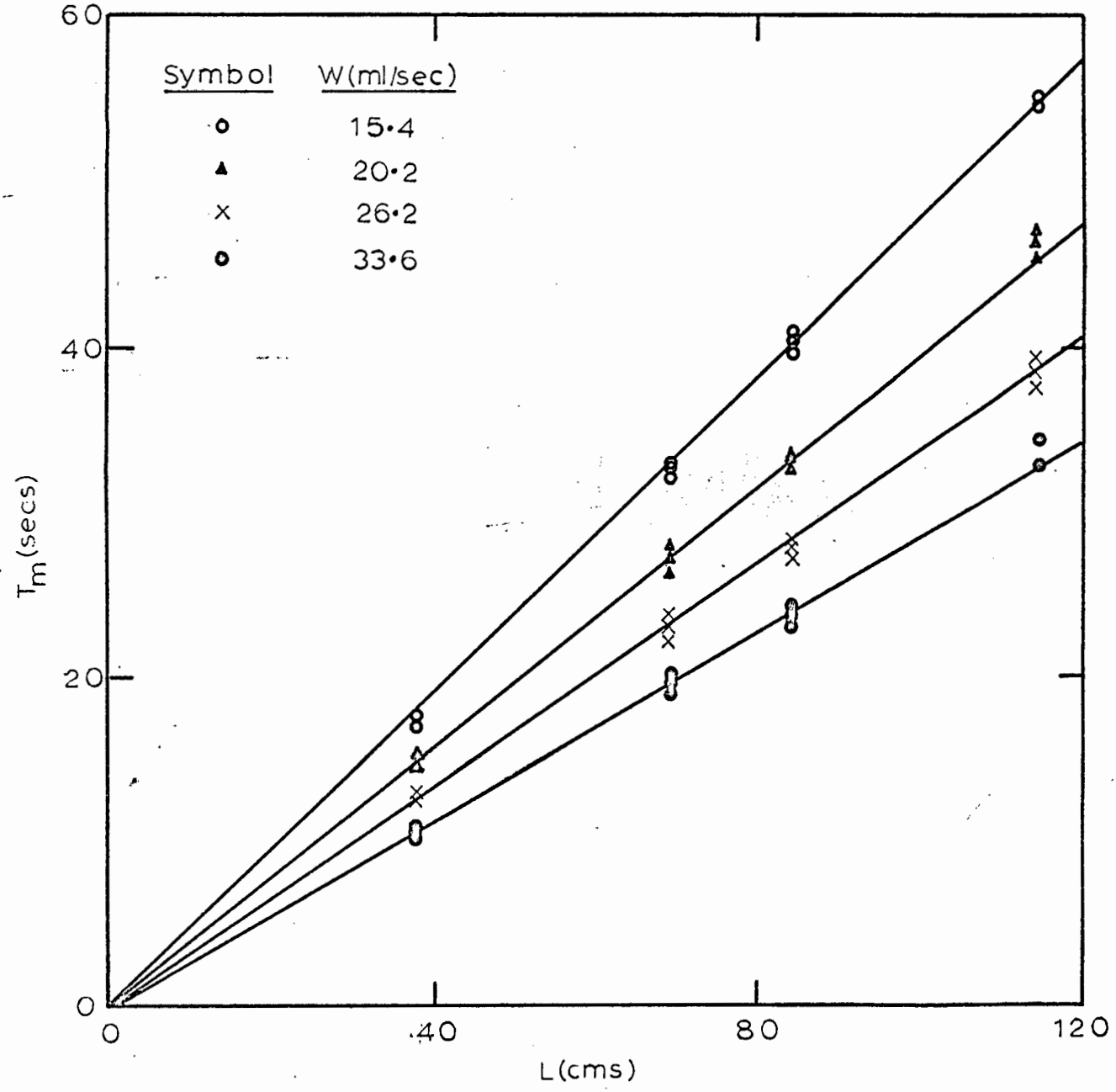

FIGURE 6(a)

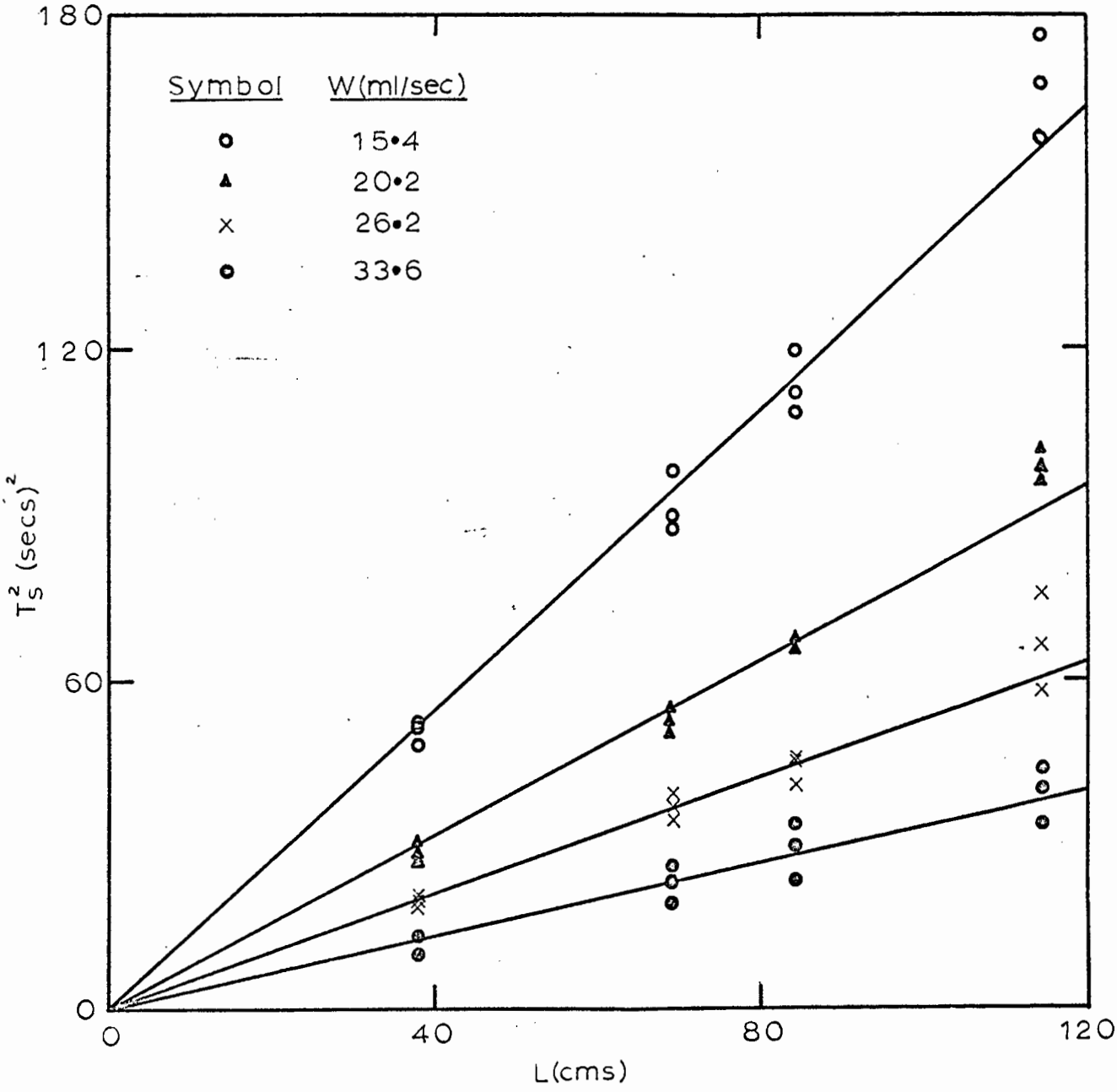
180
120
60
0
0
40
80
120
T_S^2 (secs)^2
L(cms)
Symbol
W(ml/sec)
15•4
20•2
26•2
33•6

FIGURE 6(b)

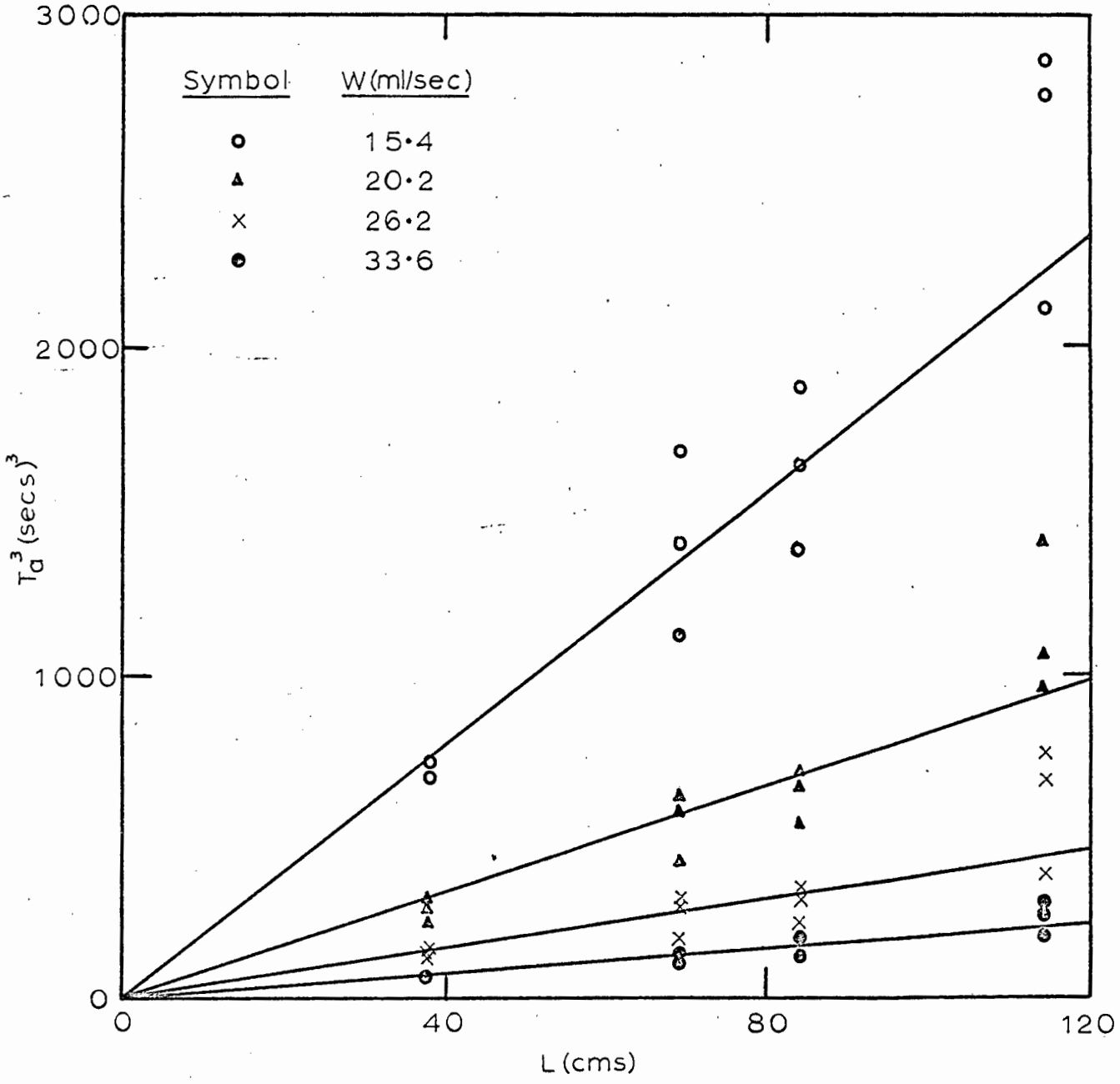
Symbol
W(ml/sec)
15·4
20·2
26·2
33·6
3000
2000
1000
0
T_a^3 (secs)^3
0
40
80
120
L (cms)

FIGURE 6(c)

equations:

$$T_m = P_1 L \quad (2.152)$$

$$T_s^2 = P_2 L^2 \quad (2.153)$$

$$T_a^3 = P_3 L^3 \quad (2.154)$$

The values of P_1, P_2 and P_3 as determined from the graphical plots are tabulated below.

TABLE 3

WATER RATE (ml./sec.)	P_1 (sec/cm)	P_2 (sec^2/cm)	P_3 ($sec.^3$/cm)
15.4	.472	1.34	19.8
20.2	.396	.79	8.1
26.2	.331	.52	3.8
33.6	.280	.35	1.9

Table 4 contains the results of the seven point radial residence time distribution measurements. A_r is the fraction of the total flow leaving the outlet of the r th cell.

TABLE 4

RUN NO.	WATER RATE (ml/sec)	PACKED HEIGHT (cms)	RADIAL POSN.	A_r	T_{mr} (secs)	T_{sr}^2 (sec^2)	T_{cr}^3 (sec^3)	ϕ
49			1	.047	12.8	36.7	346	3.29
50			2	.057	13.1	38.1	348	3.14
51			3	.048	18.1	67.0	823	3.32
52	15.4	30.5	4	.079	15.1	55.2	708	3.51
53			5	.041	17.1	63.8	728	3.06
54			6	.088	15.8	60.9	831	3.54
55			7	.111	14.8	49.9	520	3.09
56			1	.052	10.2	19.2	122	3.37
57			2	.070	10.0	18.7	141	4.03
58			3	.045	13.7	30.5	248	3.65
59	20.2	30.5	4	.065	10.9	20.4	134	3.51
60			5	.068	13.1	30.4	246	3.49
61			6	.074	10.8	19.8	131	3.61
62			7	.095	11.6	23.3	158	3.38
63			1	.069	8.9	12.8	61.3	3.33
64			2	.067	8.8	12.3	70.3	4.10
65			3	.052	11.0	15.4	72.9	3.38
66	26.2	30.5	4	.058	9.7	14.6	84.6	3.85
67			5	.073	10.7	16.3	83.2	3.35
68			6	.068	9.7	13.9	68.9	3.46
69			7	.088	9.1	12.0	62.3	3.94

70			1	.066	7.8	8.8	34.9	3.52
71			2	.065	8.0	9.8	43.2	3.60
72			3	.050	8.6	9.3	31.7	3.15
73	33.6	30.5	4	.050	8.4	9.6	37.5	3.42
74			5	.071	8.8	10.3	42.9	3.56
75			6	.070	8.3	9.9	45.1	3.82
76			7	.082	8.0	9.1	43.2	4.09
77			1	.004	39.3	135.4	1941	4.16
78			2	.006	33.9	82.0	877	4.42
79			3	.103	35.1	87.8	955	4.35
80	15.4	76	4	.020	37.4	129.5	1861	4.15
81			5	.007	35.6	119.8	1988	4.93
82			6	.165	36.5	103.9	1428	4.83
83			7	.104	34.3	101.0	1228	4.13
84			1	.019	30.2	75.7	791	4.17
85			2	.012	27.5	57.8	706	5.81
86			3	.084	29.3	64.6	668	4.69
87	20.2	76	4	.022	31.1	78.0	808	4.13
88			5	.011	26.4	43.3	369	5.20
89			6	.196	30.1	57.5	556	5.06
90			7	.092	26.7	51.9	439	4.35

91			1	.021	25.6	46.4	357	4.25
92			2	.008	25.0	43.0	305	4.13
93			3	.084	27.2	40.5	298	4.95
94	26.2	76	4	.022	27.2	42.0	287	4.43
95			5	.028	24.4	37.6	286	4.94
96			6	.180	25.4	39.1	248	4.12
97			7	.095	24.0	40.1	277	4.13
98			1	.026	21.8	28.3	178	4.84
99			2	.010	20.9	25.8	152	4.76
100			3	.076	22.8	25.0	137	4.99
101	33.6	76	4	.020	23.6	26.6	145	4.83
102			5	.070	21.0	24.3	145	5.17
103			6	.163	21.6	24.7	142	5.03
104			7	.090	20.8	24.9	146	4.89

2.7 ANALYSIS OF RESULTS

2.71 General

The results of the single outlet measurements indicate a fairly close fit to straight line relationships as can be seen from Figures 6(a), 6(b) and 6(c). According to equations (2.143), (2.144) and (2.145) this should be true only if b_2, c_2 and c_3 are negligible. To estimate the values of these parameters the radial measurements will be used.

If the assumption is made that the seven point radial moments which have been determined are representative of all the flow streams at the base of the tower, then the various summations can be performed with $n = 7$ and A_r replaced by $A_r / \sum_{r=1}^{7} A_r$. The latter has the effect of modifying A_r so that it becomes the flow rate of liquid in the r th channel divided by the combined flow rate collected from the seven cells. Substituting the values from Table 4 in the set of equations from (2.146) to (2.151) produces the results tabulated below.

TABLE 5

RUN NOS.	a_1 (sec/cm.)	b_1 (sec^2/cm)	b_2 (sec^2/cm^2)	c_1 (sec^3/cm)	c_2 (sec^3/cm^2)	c_3 (sec^3/cm^3)
49 - 55	.498	1.739	.0025	20.34	.045	.0000
56 - 62	.374	0.752	.0036	5.42	-.009	-.0015
63 - 69	.316	0.452	.0008	2.34	.004	.0000
70 - 76	.270	.313	.0001	1.32	.000	.0000
77 - 83	.469	1.324	.0002	16.92	.003	-.0002
84 - 90	.383	0.779	.0003	7.57	.003	.0000
91 - 97	.335	0.527	.0010	3.61	.000	-.0005
98 - 104	.285	0.330	.0001	1.90	.000	.0000

The above table indicates that b_2 , c_2 and c_3 are small and, therefore we can write:

$$T_m \approx a_1 L \quad (2.155)$$

$$T_s^2 \approx b_1 L \quad (2.156)$$

$$T_a^3 \approx c_1 L \quad (2.157)$$

which agrees with the results of run numbers 1 to 48.

It would be of interest to compare the above values of a_1 , b_1 and c_1 with those of P_1 , P_2 and P_3 determined from the slopes of the graphical plots for the moments of the single outlet runs. This will give an indication of the degree to which the seven points analysed are representative of the entire cross-section at the base of the packing. In the table below a_1 , b_1 and c_1 are the average values for the two heights of packing used.

TABLE 6

WATER RATE (ml/sec)	P_1 (sec/cm)	a_1 (sec/cm)	P_2 (sec^2/cm)	b_1 (sec^2/cm)	P_3 (sec^3/cm)	c_1 (sec^3/cm)
15.4	.472	.484	1.34	1.53	19.8	18.6
20.2	.396	.379	0.79	0.77	8.1	6.5
26.2	.331	.326	0.52	0.49	3.8	3.0
33.6	.280	.278	0.35	0.32	1.9	1.6

Considering that less than half the total flow from the packed section was collected by the seven cells, the results above show surprisingly good agreement. That the measurements made were fairly representative of the cross-section as a whole is thus definitely confirmed.

2.72 Evaluation of Model A Parameters.

Equations (2.91), (2.92) and (2.93) express the moments for each stream in terms of the parameters of Model A. As this model involves only two parameters for each stream, i.e. $\bar{u}_r$ and D_r, these can be evaluated from the experimental data for T_{mr} and T_{sr}^2. The third moment was also measured and it can therefore be used to give some indication on the degree of fit of the model. This can be most conveniently done by applying the result of equation (2.95), where the ratio ϕ is found to be 3. It can be seen from Table 4 that the experimental values of ϕ are reasonably close to this theoretical value for a packed height of 30.5 cms., but for the higher height of 76 cms. a larger deviation exists. It should be stressed that ϕ is very sensitive to small changes in the distribution curve, especially when analysing a system which is close to plug flow; as is the case with the present study. This point is illustrated in Appendix 1.4.

From equation (2.91),

$$\bar{u}_r = L / T_{mr} \qquad (2.158)$$

TABLE 7

BED HEIGHT L (cms)	WATER RATE W (ml/sec)	$\bar{u}_r$ (cm/sec) RADIAL POSITION						
		1	2	3	4	5	6	7
30.05	15.4	2.38	2.33	1.69	2.02	1.78	1.93	2.06
	20.2	2.99	3.05	2.22	2.80	2.33	2.82	2.63
	26.2	3.43	3.47	2.77	3.14	2.85	3.14	3.35
	33.6	3.91	3.81	3.55	3.63	3.47	3.68	3.81

(Table 7 continued)

BED HEIGHT L (cms)	WATER RATE W (ml/sec)	$\bar{u}_r$ (cm/sec)						
		RADIAL POSITION						
		1	2	3	4	5	6	7
76	15.4	1.93	2.24	2.16	2.03	2.14	2.08	2.22
	20.2	2.52	2.76	2.59	2.44	2.88	2.52	2.85
	26.2	2.97	3.04	2.79	2.79	3.11	2.99	3.16
	33.6	3.48	3.64	3.33	3.22	3.62	3.52	3.65

Comparing these results with those for A_r in Table 4, there appears to be no correlation between this quantity and $\bar{u}_r$ at a given flow rate and packed height. On the other hand a distinct relationship exists between $\bar{u}_r$ and W. This trend is particularly interesting for the packed height of 30.5 cms., where the form of the correlation varies with radial position. Letting

$$\bar{u}_r = AW^b \qquad (2.159)$$

the values of A and b can be determined from a log-log plot as shown in Fig.7(a). To avoid confusion only two lines are drawn through the data. A summary of the results is given in Table 8. Their significance will be discussed in Section 2.74.

TABLE 8

RADIAL POSITION	AVERAGE A_r	A	b
1	0.059	0.63	0.70
2	0.065	0.36	0.70
3	0.049	0.13	0.93
4	0.063	0.33	0.69
5	0.063	0.18	0.85
6	0.075	0.33	0.69
7	0.094	0.22	0.82

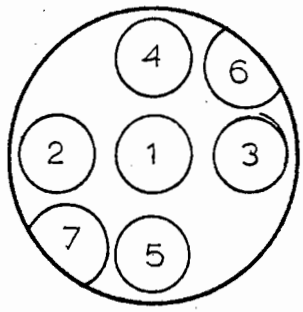

symbol	r
o	1
×	2
Δ	3
●	4
⊖	5
⊘	6
⌀	7

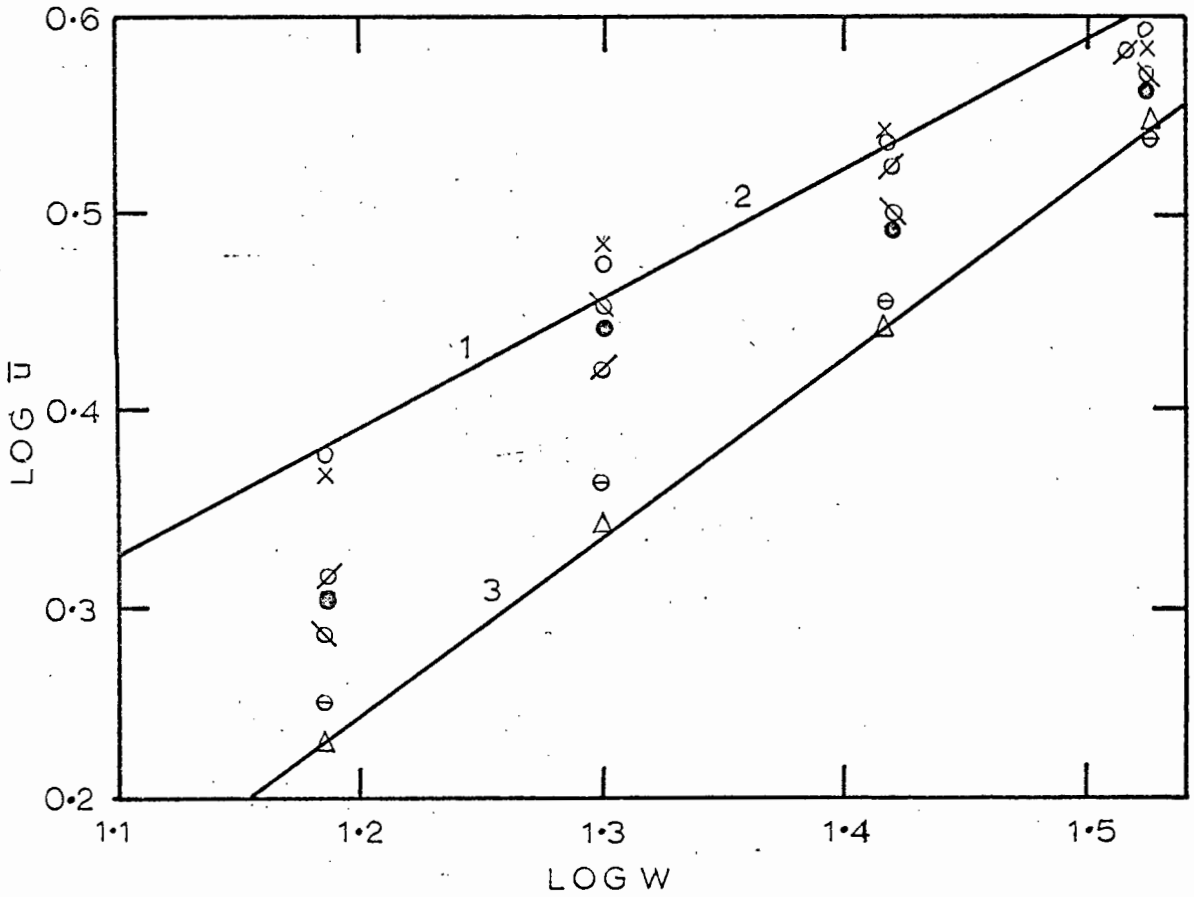

FIGURE 7(a)

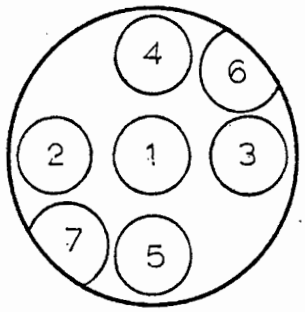

symbol	r
o	1
×	2
Δ	3
⊛	4
⊖	5
⊗	6
⌀	7

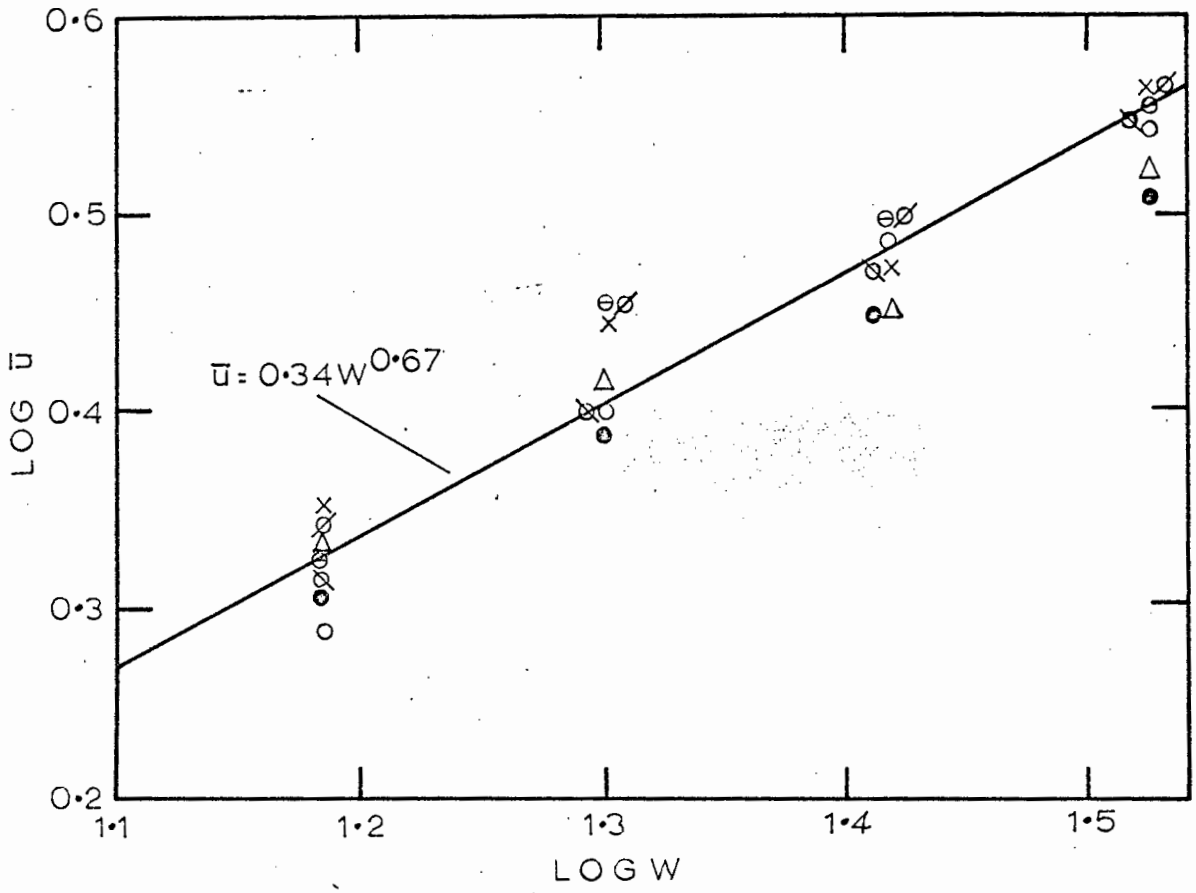

FIGURE 7(b)

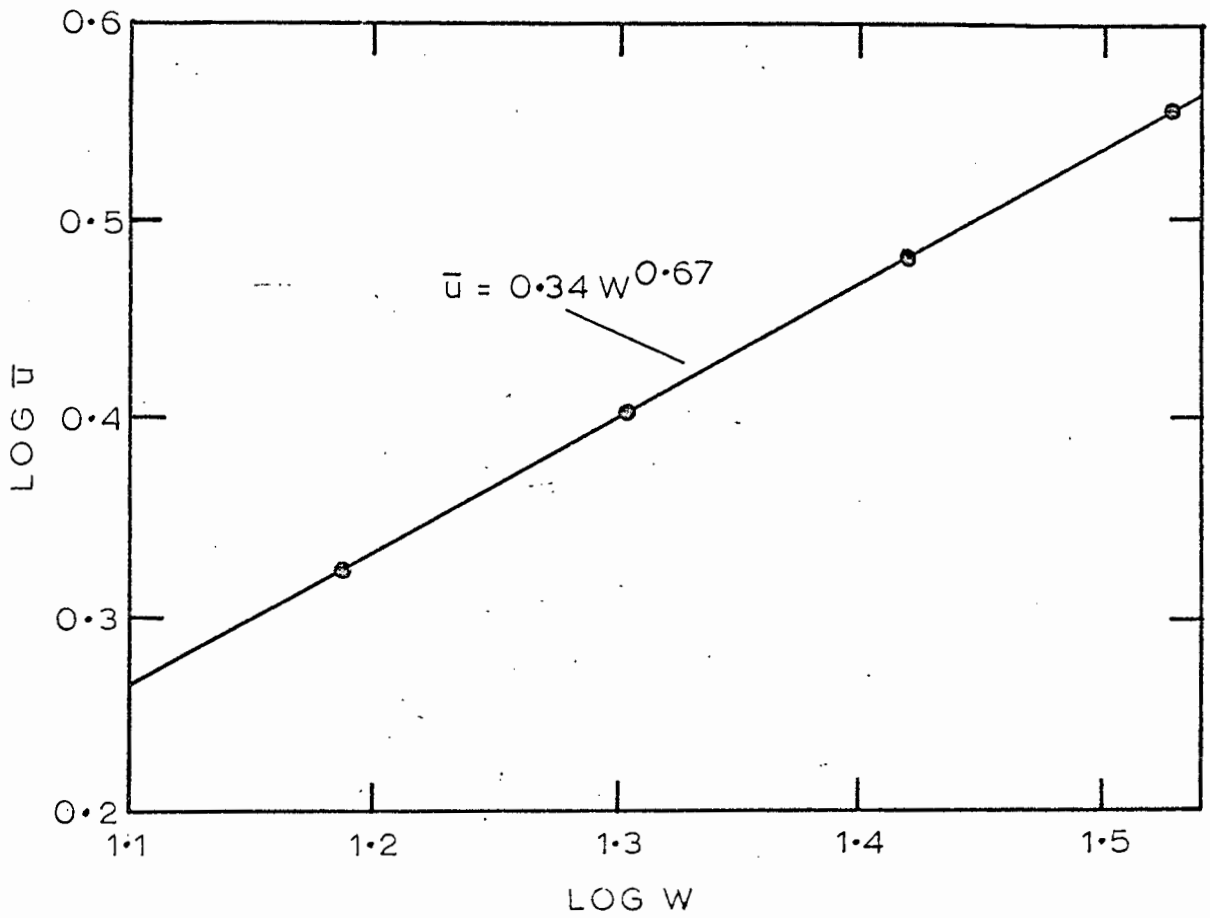

FIGURE 7(c)

For the packed height of 76 cms., the above variation is not as pronounced, as can be seen from Fig. 7(b). It would thus be expected that these results can be correlated as a whole by the same equation as for the single outlet measurements. Fig. 7(c) is a plot of log $\bar{u}$ versus log W for the latter runs, where $\bar{u}$ has been determined from the equation:

$$\bar{u} = \frac{1}{P_f} \qquad (2.160)$$

Values of P_f have been extracted from Table 3. The set of data is very well correlated by equation (2.159), with a = 0.34 and b = 0.67. In Fig. 7(b) the solid line represents the same equation. It can be seen that good agreement is obtained.

The longitudinal dispersion coefficient, D_r can be determined from equations (2.91) and (2.92):

$$D_r = \frac{L^2 T_{sr}^2}{2 T_{mr}^3} \qquad (2.161)$$

TABLE 9

Bed Height L (cms)	Water Rate W (ml/sec)	D_r (cm²/sec) RADIAL POSITION						
		1	2	3	4	5	6	7
30.5	15.4	8.13	7.87	5.26	7.44	5.93	7.17	7.14
	20.2	8.42	8.70	5.52	7.30	6.28	7.31	6.95
	26.2	8.44	8.41	5.38	7.44	7.21	7.08	7.41
	33.6	8.63	8.90	6.80	7.54	7.02	8.06	9.26
76	15.4	6.43	6.07	5.86	7.16	7.67	6.17	7.22
	20.2	7.92	8.03	7.43	7.51	6.80	6.08	7.89
	26.2	7.98	7.96	5.82	6.03	7.44	6.89	9.39
	33.6	7.86	8.19	6.07	5.82	7.55	7.06	8.99

The values for each position show only small variations with W. There is a general trend for Dr to increase with increasing flow rate, but a larger range of W would be necessary to enable a more conclusive correlation to be proposed.

According to equation (2.66), the effective axial diffusion coefficient for the single outlet runs should be proportional to $(\bar{u})^{\frac{1}{2}}$. Fig.8 illustrates that reasonable agreement is obtained. The values of D and $\bar{u}$ have been calculated from the results in Table 2 according to the equations:

$$D = \frac{L^2 T_s^2}{2 T_m^3} \qquad (2.162)$$

and

$$\bar{u} = L/T_m \qquad (2.163)$$

2.73 Evaluation of Model B parameter.

The parameter of Model B which is of most interest is x', the height of film between mixing points. From equation (2.129) and (2.130),

$$x' = \frac{B_1 T_{sr}^2 \bar{u}_r Z'}{B_2 T_{mr} (1 - Z')} \qquad (2.164)$$

Z', B_1 and B_2 were determined from the computer results of the program in Appendix 2.2, when the value of $B_1 B_3 / B_2^2$ was the same as the experimental value of ϕ .

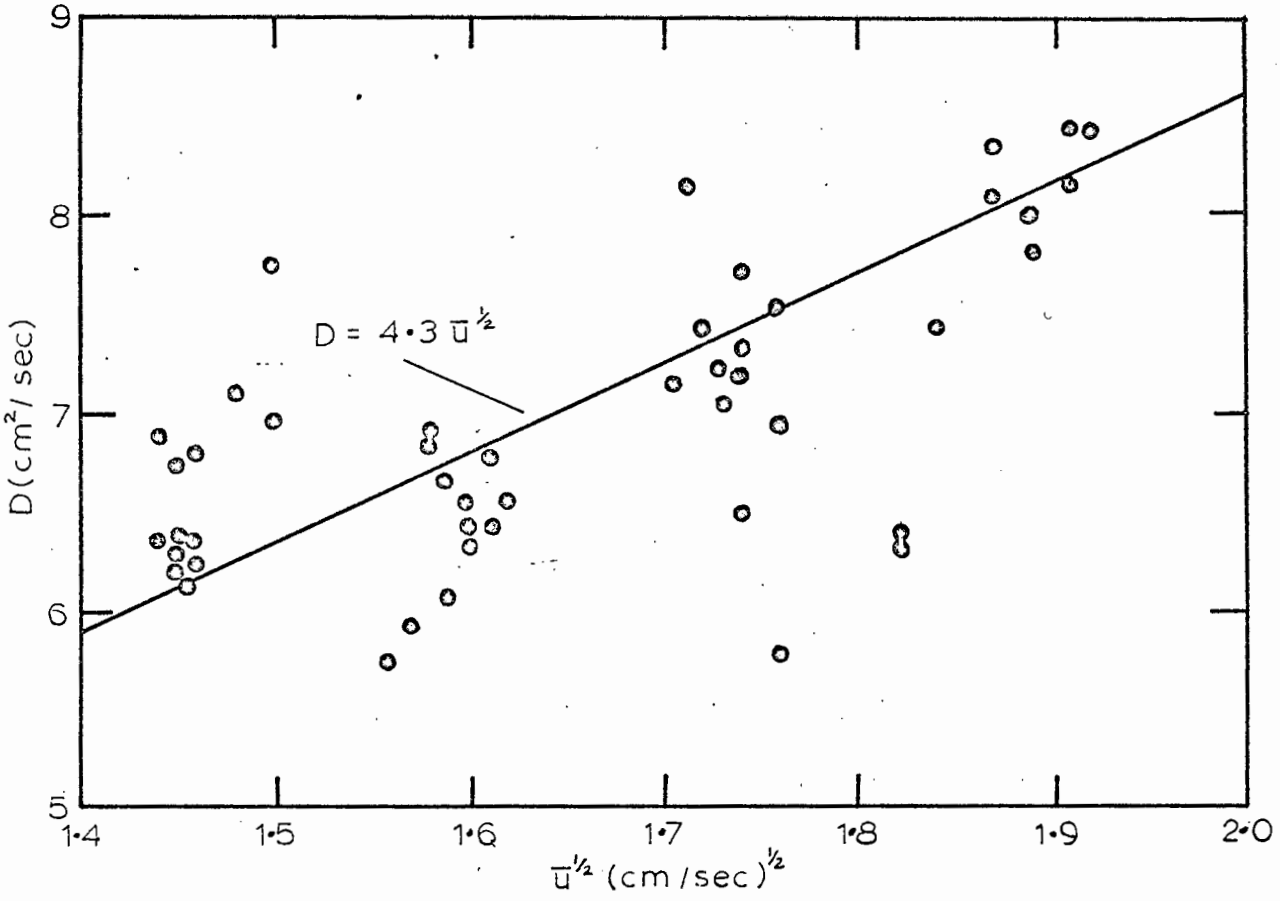

FIGURE 8

TABLE 10

BED HEIGHT L (cms)	WATER RATE W (ml/sec)	x^1 (cms) RADIAL POSITION 1	2	3	4	5	6	7
30.5	15.4	50.2	48.9	44.7	52.3	48.1	52.4	50.4
	20.2	40.1	39.0	34.6	37.1	38.2	36.3	37.6
	26.2	35.3	33.1	27.6	32.8	31.1	31.9	30.4
	33.6	31.2	32.9	27.6	29.4	28.7	30.4	29.6
76	15.4	45.2	36.3	36.3	47.7	46.7	38.7	44.4
	20.2	42.8	35.6	37.6	41.7	30.0	31.0	37.1
	26.2	36.2	35.6	26.9	28.7	31.0	31.4	36.0
	33.6	29.4	29.3	23.6	23.7	26.8	25.8	28.4

The results are presented graphically in Figs. 9(a) and 9(b). The same trend as was found in the case of $\overline{v}_r$ is again present here. At the packed height of 30.5 cms. a variation of x^1 according to radial position is evident, whereas for 76 cms. this is not as marked. The results for the former also show a tendency to flatten off to a constant value at the highest flow rate used. The latter do not exhibit this tendency to the same degree.

2.74 Discussion

The results of the radial point measurements have shown that the moments of the residence time distribution curves do vary from one point to another at the base of a given packed section. The analysis in Section 2.71, however, indicates that this variation has only a small effect on the moments

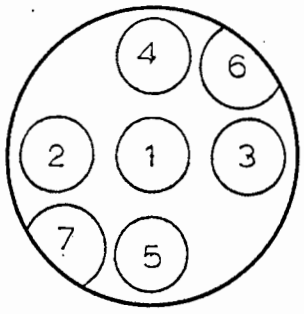

symbol	r
o	1
×	2
Δ	3
⊙	4
⊖	5
⊘	6
⌀	7

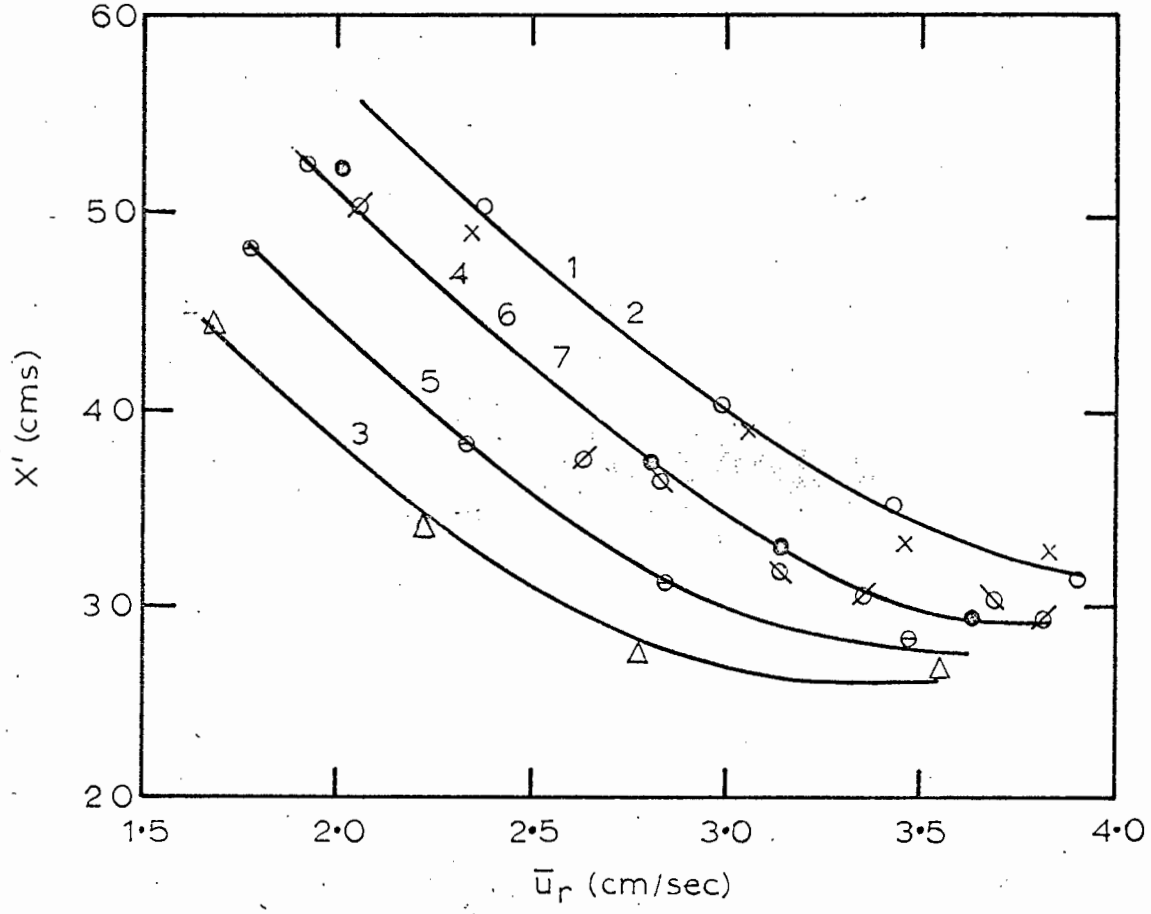

FIGURE 9(a)

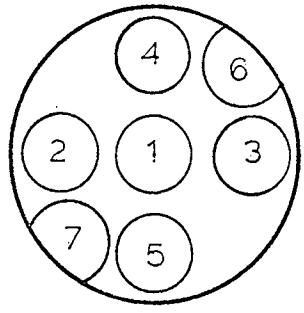

symbol	r
o	1
×	2
Δ	3
⊙	4
⊖	5
⊗	6
⊘	7

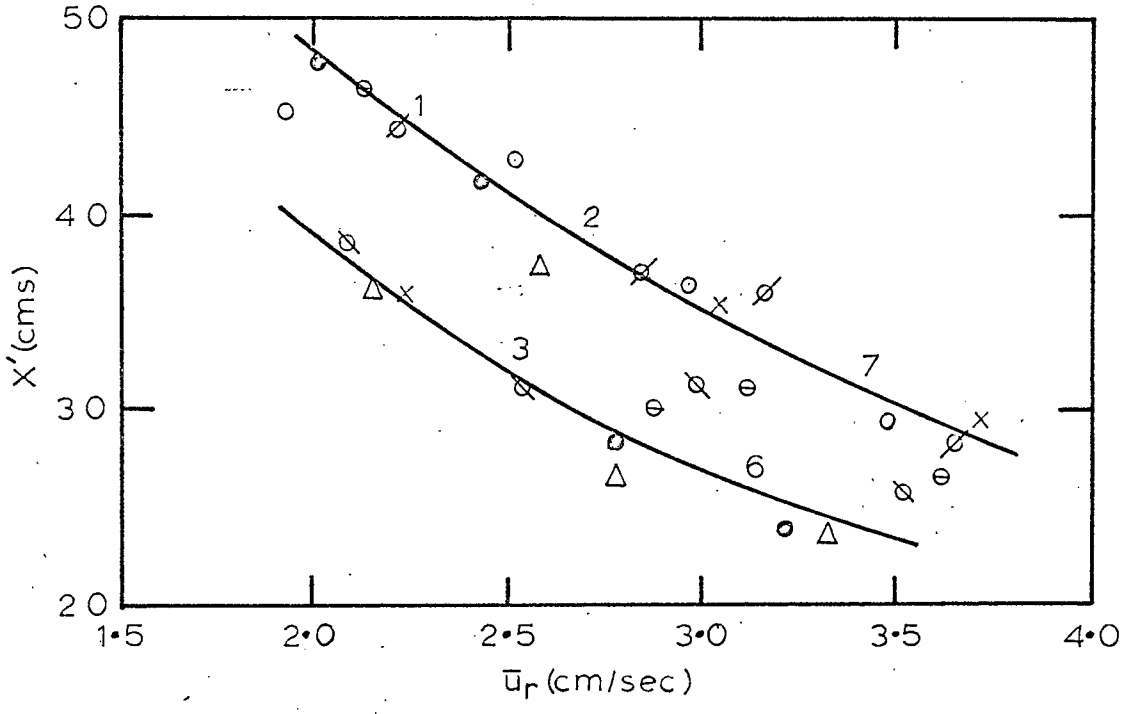

FIGURE 9(b)

of the curve which is obtained when all the individual streams are combined. The conclusion one can draw from this is that, unless its limitations are realised, disturbance testing with a single outlet measuring point could give a completely misleading picture of the hydrodynamic conditions.

The analysis of the flow models introduced in this study has produced a number of interesting features. The parameter which is common to both, i.e. $\bar{u}_r$, has been shown to fit a correlation of the form of equation (2.159). The value of b in this equation was found to vary from one stream to another, particularly for a bed height of 30.5 cms. If a stream behaved as an ideal laminar film flowing down a flat plate[52], b would have the value of $\frac{2}{3}$, whereas if it were totally enclosed by solid boundaries, b would be equal to 1. Table 8 shows that all the experimental measurements for b lie between these two values. One may infer from this that initially some of the streams consist of partially enclosed channels due to the high local flow rate at points in the vicinity of the column inlet. As the liquid passes down the bed, however, it is dispersed by the packing to form a more even radial distribution. Under these conditions film-type flow should prevail. Thus we find that b is very close to the theoretical value of $\frac{2}{3}$ for the packed height of 76 cms.

There is also the possibility that a fair amount of cross-flow takes place between the various axial channels in the bed. This would explain why the values of $\bar{u}_r$ and x' for 30.5 cms. bed height show far larger variations from one radial point to another than those for 76 cms. The cross-flow would cause the individual streams to lose their identity to a certain degree as the axial flow paths lengthen. The results in Table 5 tend to support this theory as the values of b_2 and c_2 are found in most cases to be higher for the packed height of 30.5 cms.

2.8 APPLICATIONS OF MODELS TO LIQUID SIDE MASS TRANSFER STUDIES

2.81 Correction of mass transfer coefficient for non-ideal behaviour of the liquid side.

It is intended to determine the effect of non-plug flow behaviour of the liquid stream on a simple absorption process. Model A will be used to analyse this effect as numerical methods of solution are not necessary when it is applied to the case of a first order absorption mechanism. An example of this is the physical absorption of a pure gas, such as carbon dioxide with water as solvent.

$$\text{Rate of absorption} = k_l a\,(Ce - C) = k_l a\,C' \qquad (2.165)$$

where $C' = C - C_e$ (2.166)

As in the case of a first order reaction[53] :

$$\frac{C_f'}{C_o'} = \int_0^\infty e^{-k_l a t} E(t)\,dt \qquad (2.167)$$

$$= \Big[E(s)\Big]_{s = k_l a} = \Big[G(s)\Big]_{s = k_l a} \qquad (2.168)$$

Therefore, substituting equation (2.89)

$$\frac{C_f'}{C_o'} = \exp\left[\frac{\bar{u}L}{2D} - \sqrt{\frac{\bar{u}^2L^2}{4D^2} + \frac{k_l a L^2}{D}}\right] \qquad (2.169)$$

Solving for $k_l a$,

$$k_l a = \frac{D\left(\ln \frac{C_f'}{C_o'}\right)^2}{L^2} - \frac{\bar{u}}{L} \ln \frac{C_f'}{C_o'} \qquad (2.170)$$

If plug flow is assumed, then for the same amount absorbed,

$$\frac{C_f'}{C_o'} = \exp\left(-k_l' a \, L/\bar{u}\right) \qquad (2.171)$$

where $k_l' a$ is the mass transfer coefficient on the assumption of plug flow.

$$\ln \frac{C_f'}{C_o'} = -k_l' a \, L/\bar{u} \qquad (2.172)$$

Substituting in (2.170)

$$\frac{k_l a}{k_l' a} = 1 + \frac{D k_l' a}{\bar{u}^2} \qquad (2.173)$$

Values of $k_l' a$ have been estimated from the data of Sherwood and Holloway for berl saddles. Unfortunately these workers did not use $\frac{1}{4}$" saddles, but the estimated values will serve to illustrate the principles involved.

For model A,

$$\frac{D}{\bar{u}^2} = \frac{1}{2} \frac{T_s^2}{T_m} = \frac{1}{2} \frac{P_2}{P_1} \qquad (2.174)$$

TABLE 11

W (ml/sec)	$D/\bar{v}^2$ (sec)	$k_l'a$ (sec^{-1})	$\frac{k_l'a}{k_l'a}$
15.4	1.42	.0119	1.0169
20.2	1.00	.0147	1.0147
26.2	0.79	.0172	1.0136
33.6	0.62	.0194	1.0120

The results in Table 11 indicate that errors of between 1% and 2% can be expected for this system. It would thus appear that the assumption of plug flow is a fairly good one for slow processes such as physical absorption. However, it is obvious from equation (2.173) that the faster the absorption rate, the larger will be the error involved. It is possible, therefore, that in cases where the rate of absorption is enhanced by the presence of a chemical reaction in the liquid phase, the assumption of plug flow may lead to serious errors in the evaluation of the mass transfer coefficients. This factor could be a contributary cause to the present lack of success in the theoretical analysis of such data. By applying Model A in a similar fashion as above, it is possible to correct the data as presented by investigators who have assumed ideal flow conditions in their equipment. At present, however, there is insufficient residence time distribution data to formulate a general correlation for D. It is advisable, therefore, that disturbance testing should be performed in conjunction with mass transfer studies to enable the correction to be made.

2.82 Prediction of k_l from Model B

As indicated in Section 2.41, Model B was introduced in an attempt to estimate the mass transfer coefficient, k_l from disturbance measurements. The absorption of carbon dioxide in water is again chosen as an example. It will be seen that the value calculated in this manner is considerably lower than the mass transfer data would suggest. Exact comparison is difficult as this would require the interfacial area to be known and as present experimental values for this quantity are uncertain only an order of magnitude discrepancy between the mass transfer measurements and the results for Model B will be calculated.

According to the penetration theory of Higbie, the mass transfer coefficient for physical absorption is[2] :

$$k_l^* = \sqrt{\frac{D'}{\pi\,\theta}} \qquad (2.175)$$

where D' = molecular diffusivity of the gas in the solvent and θ = exposure time between mixing.

As we are only interested in approximate values, θ will be taken as $x'/\bar{u}$. Using the values of x' and $\bar{u}$ from Section 2.7, an estimated interfacial area from Shulman et al[11] and with $D' = 1.77 \times 10^{-5}$ cm /sec[19] for CO_2 in water, Table 12 can be compiled. The experimental results of Sherwood and Holloway[16] are presented for purposes of comparison. These are the same as the k_l'a values used in Section 2.81.

TABLE 12

W (ml/sec)	θ (secs)	$\sqrt{\frac{D'}{\pi\theta}} \times 10^4$ (cm/sec)	$k^*_l a \times 10^4$ (sec^{-1})	$k_l' a \times 10^4$ (sec^{-1})	$\frac{k_l' a}{k_l^* a}$
15.4	18.1	5.58	1.83	119	65
20.2	12.8	6.63	2.33	147	63
26.2	10.3	7.40	2.77	172	62
33.6	8.4	8.19	3.22	194	60

The ratio in the last column of the table above indicates that bulk mixing as described by Model B, has very little influence on the rate of mass transfer. It could be that Model B gives a completely incorrect picture of the mechanism of tracer dispersion in the film. On the other hand, however, it seems highly feasible that the interfacial layers are mixed far more frequently than those deeper in the film. The result of this would be to give an apparent average mixed length much larger than that existing in a localised region near the interface.

2.9 CONCLUSIONS

The techniques introduced in measuring and analysing the response of a physical flow system to a dirac delta input disturbance have produced results which throw new light on the dynamic behaviour of the liquid side in a packed absorption column. The use of the moments of the distribution curve to obtain meaningful values for the parameters of the mathematical models proposed has been made possible mainly through the minimisation of errors as described in Section 2.23. The main conclusions that can be drawn from these results may be summarised as follows:

(a) The packed section consists of a number of liquid streams flowing in longitudinal channels. A significant amount of cross-flow occurs between these channels.

(b) The liquid in each stream flows over the packing in the form of a film. Laminar flow in the film is closely approached but a certain amount of mixing does occur. This agitation appears to take place predominantly in the vicinity of the gas/liquid interface.

Nomenclature for Section 2.

A	-	parametric constant in eqn. (2.159)
A_o A_1	-	parametric constants in eqn. (2.67)
A_r	-	fraction of total flow rate in r th stream.
a	-	gas/liquid interfacial area per unit volume of tower.
a_1	-	parametric constant in eqn. (2.146)
B_1 , B_2 , B_3	-	defined by eqns. (2.126), (2.127), (2.128) resp.
b	-	parametric constant in eqn. (2.159)
b_1 , b_2	-	parametric constant in eqns. (2.147), (2.148) resp.
$C(t)$	-	concentration of tracer in outlet at time t
C_r	-	concentration of tracer in r th stream
C_e	-	saturated concentration of gas in liquid
C_f	-	final concentration of gas in liquid minus saturated concentration.
C'_o	-	initial concentration of gas in liquid minus saturated concentration.
C_1 , C_2 , C_3	-	parametric constants in eqns. (2.149), (2.150), (2.151) resp.
D	-	effective axial diffusion coefficient.
D_r	-	effective axial diffusion coefficient for liquid in r th stream.
D'	-	molecular diffusion coefficient of gas in liquid.
d_p	-	effective diameter of packing piece.
$E(t)$	-	external age distribution function.
$F(t)$	-	defined by eqn. (2.2)
$F(s)$	-	La Place Transformation of f (t) as defined by eqn. (2.19)
$f(t)$	-	arbitrary function of t.
$G(s)$	-	arbitrary transfer function of a system
g	-	acceleration due to gravity

H	-	parameter of Model B as defined by eqn. (2.118)
	-	holdback as defined by eqn. (2.1)
k_l	-	liquid side mass transfer coefficient
k'_l	-	mass transfer coefficient assuming plug flow on liquid side
k^*_l	-	mass transfer coefficient from Model B
L	-	height of packing
m	-	parameter of Model B
n	-	total number of axial streams in a packed section.
P_1, P_2, P_3	-	parametric constants in eqns. (2.152), (2.153), (2.154) resp.
p	-	La Place Transform variable of x
Q	-	constant in eqn. (2.57)
q	-	label indicating moment number
	-	number of mixing sections in a bed length L.
R	-	constant in eqn.(2.57)
r	-	label indicating axial stream number
S	-	segregation as defined by eqn. (2.3)
s	-	La Place Transform variable of t.
T_m	-	mean residence time defined by eqn. (2.6)
T_s	-	spread of distribution curve about the mean as defined by eqn. (2.7).
T_a	-	skewness of distribution curve about the mean as defined by eqn. (2.8)
t	-	independent time variable
t_1	-	break-away point on residence time distribution curve.
t_n	-	return point on residence time distribution curve
t_c	-	defined by eqn. (2.4)
$\bar{v}_r$	-	point axial velocity in r th stream

$\bar{u}_r$ - mean axial velocity in r th stream.

$\bar{u}$ - average axial velocity of liquid in bed.

W_r - defined by eqn. (2.100)

W - water flow rate

x - independent variable denoting axial distance.

x' - length of film between mixing points.

y - independent variable denoting distance into the film from gas/liquid interface.

Z - defined by eqn. (2.119)

Z' - defined by eqn. (2.121)

α_0 α_1 α_2 α_3 - moments of distribution curve as defined by eqns. (2.16), (2.17), (2.18) and (2.19) resp.

β_0 β_1 β_2 - defined by eqns. (2.79), (2.80) and (2.81) resp.

γ_1 - coefficient of variance as defined by eqn. (2.67).

δ - defined by $\delta = \ln \alpha_0$

ζ_q - error in q th moment

ϵ - error in determining E (t)

θ - exposure time between mixing points

θ_i - arbitrary input signal

θ_o - arbitrary output signal

μ - viscosity of liquid

ρ - density of liquid

τ^* - time axis about which moments must be taken for minimum error.

τ_q - q th moment of distribution curve about time axis τ^*

ϕ - moment ratio as defined by eqn. (2.94).

* * *

SECTION 3

CHEMICAL REACTION STUDIES

3.1 INTRODUCTION

The effects of deviations from the two ideal models, namely plug flow and the continuous stirred tank, on the conversion of a chemical reaction has recently been the subject of many theoretical investigations[30]. However, even in the case of a simple first order irreversible reaction, very little has been done experimentally to verify the theories proposed.

For the first order irreversible reaction $A \xrightarrow{k'} R$,

$$\frac{C_{Af}}{C_{Ao}} = \int_0^\infty e^{-k't} \, E(t) \, dt \qquad (3.1)$$

where C_{Ao} is the initial concentration of A

C_{Af} is the final concentration of A

k' is the reaction velocity constant

and $E(t)$ is the external age distribution function[30].

The conversion for this type of reaction can, therefore, be calculated

directly from the results of pulse testing. In the case of a second order reaction, however, additional information is necessary[30]. Consider the reaction

$$A + B \xrightarrow{k} P + R.$$

To predict the outlet concentrations of A and B it would be necessary to know their concentrations at all points within the system. If a particular flow model is chosen which describes exactly the position of each element of fluid as it passes through the system, then it would be expected that the model would predict the conversion that would be obtained experimentally in the physical system. As it is possible that the external age distribution of many mathematical models can be approximated to the measured distribution with almost equal degree of fit in each case, the conversion for a second order reaction may differ for each model. The experimental determination of conversion for such a reaction in a flow system could, therefore, be a useful means of closing a model from among those which have similar residence time distribution curves.

In selecting a reaction to perform in a particular system, the following factors will have to be taken into consideration.

(a) The reaction must be fairly rapid. As was illustrated in Section 2.81, non-ideal flow effects are more significant the faster the reaction rate.

(b) The reaction must be one which has been exhaustively tested and whose kinetics are firmly established.

(c) The analysis of samples must be quick and simple to perform.

The reaction chosen was the saporification of ethyl acetate by sodium hydroxide.

$$EtOAc + NaOH \rightarrow EtOH + NaOAc$$

This reaction has been studied by many workers and the rate equation has been conclusively proved as being that of the second order and irreversible.[49]

$$r = k C_A C_B \qquad (3.2)$$

where C_A = concentration of ethyl acetate
and C_B = concentration of sodium hydroxide

3.2 APPARATUS AND EXPERIMENTAL PROCEDURE

The same column was used as for the pulse testing, but inlet and outlet positions were modified as shown in Fig.10. It was essential that the mixture of sodium hydroxide and ethyl acetate be introduced before much reaction could take place. At the same time the two liquids must be well mixed. The inclusion of a mixer in the inlet stream would inevitably have resulted in excessive pre-conversion. It was decided to rely on a number of sudden changes in the direction of the liquid stream to perform the function of mixing.

At the base of the column, the collecting and analysing technique has to be both rapid and accurate. The former is extremely important as the

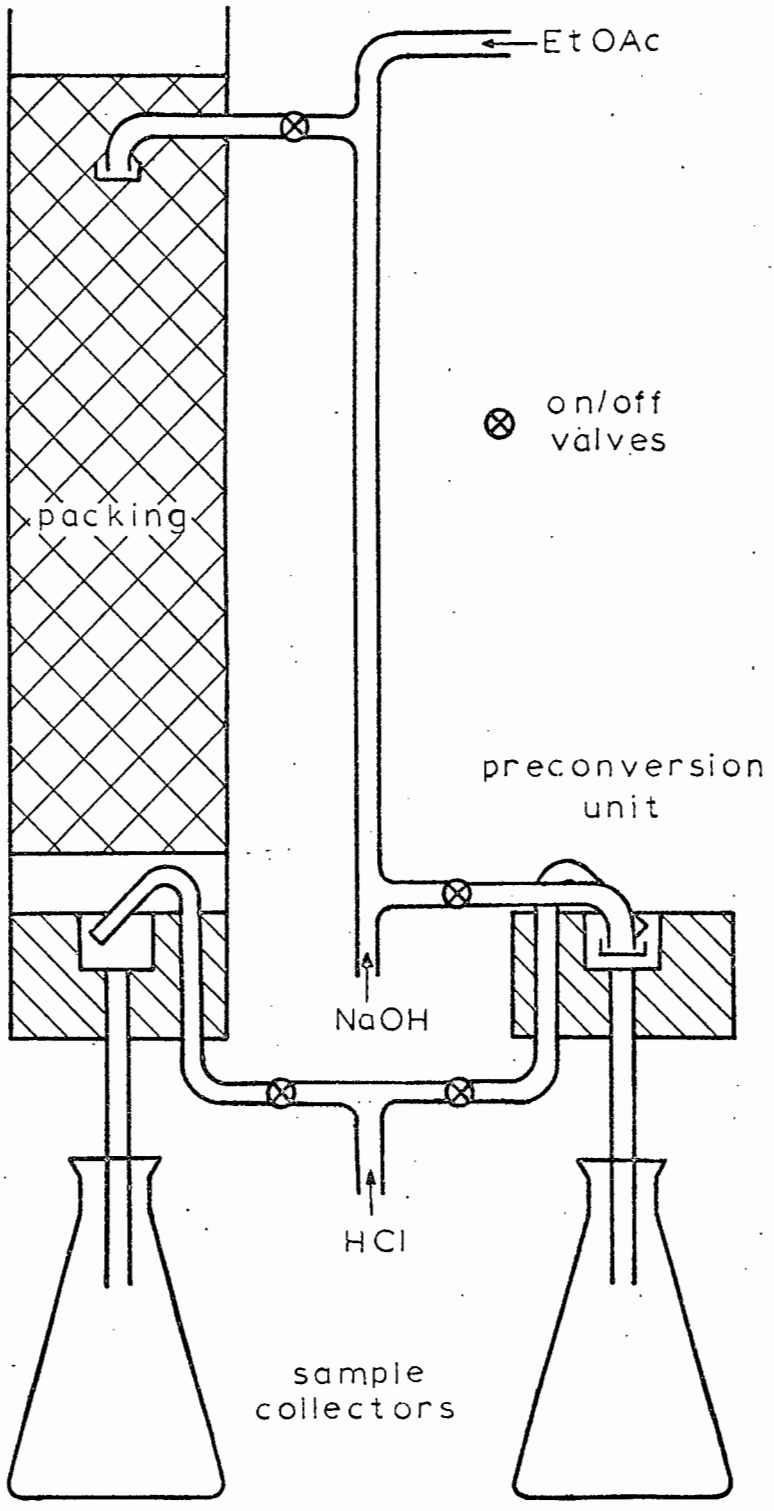
EtOAc
on/off valves
packing
preconversion unit
NaOH
HCl
sample collectors

FIGURE 10

reaction rate is high and the loss of a second in time between collecting and analysing would have introduced a significant error in the runs performed. It was therefore, necessary to halt the reaction as soon as the liquid left the bottom of the packed section. This was achieved by allowing a previously standardised solution of hydrochloric acid to mix continuously with the liquid at this point. This solution also contained phenol phthalene so that its flow rate could be adjusted to produce an almost neutral solution with the reaction products. The sample was collected as shown in Fig.10 and after exact neutralisation was analysed for unreacted ethyl acetate. To allow for the small amount of preconversion, which would be expected, a duplicate inlet and outlet arrangement was set up as shown in Fig.10. The values obtained from this device were used as the initial concentrations of the two reactants in the column calculations.

The detailed experimental procedure was as follows. With the valve system set to allow both reactants to pass into the top of the column, the flow rates of these solutions were adjusted to the required values. After about five minutes had elapsed, the flow rate (V_w ml/sec) was measured by sampling at the base of the tower over a given length of time and determining the volume collected. The temperature of this solution was also recorded. Part of the sample was then set aside and allowed to come to equilibrium conversion. This will be labelled "sample W".

After collection of sample W, the HCl solution was allowed to mix with the reaction products at the base of the tower until the colour of the liquid leaving the column was a faint pink. The volumetric flow rate (V_x ml/sec) of this stream was also measured as before. A quantity of this sample, to be labelled "sample X" was neutralised with standard HCl (this generally required only a

few drops). 50 ml. aliquots were then pipetted into stoppered flasks which, after the addition of a known excess of a standard NaOH solution, were sealed and allowed to stand for several hours before the remaining NaOH was titrated with standard HCl solution. As the concentration of NaOH was always greater than EtOAc in all the runs performed, sample W was analysed by direct titration of 50 ml. aliquots with standard HCl solution.

When the column run was completed the valves were arranged to divert the reactants to the preconversion unit. Here precisely the same procedure was adopted as for the column, the samples being labelled "sample Y" and "sample Z" where the former was for equilibrium determination purposes. The flow rates were V_y and V_z respectively.

From the stoichiometry of the reaction

$$C_B - C_A = C_{BO} - C_{AO} = C_{Bf} - C_{Af} = C_{Be} \quad (3.3)$$

C_{Be} can be determined from samples W and Y. The values of C_{BW} and C_{BY} should be identical as should V_W and V_y.

$$C_{Be} = C_{BW} = C_{BY} \quad (3.4)$$

This was found to hold very closely for all the runs performed, indicating that both the relative flow rates and concentrations of the reactants were steady for the duration of the test.

The initial and final concentrations can be determined from mass balances as follows:-

$$C_{Af} = C_{AX} \frac{V_x}{V_w} \quad (3.5)$$

$$C_{Bf} = C_{Af} + C_{Be} \quad (3.6)$$

$$C_{AO} = C_{AZ} \frac{V_z}{V_y} \quad (3.7)$$

$$C_{BO} = C_{AO} + C_{Be} \quad (3.8)$$

3.3 THEORETICAL ANALYSIS

For the second order irreversible reaction, the equations describing the concentration of reactant A are:-

(i) for Model A

$$D \frac{d^2 C_A}{dx^2} - \bar{u} \frac{d C_A}{dx} - kC_A (C_A + C_{BO} - C_{AO}) = 0 \quad (3.9)$$

(ii) for Model B: at a given value of y

$$- u(x,y) \frac{dC_A}{dx} - kC_A (C_A + C_{BO} - C_{AO}) = 0 \quad (3.10)$$

These equations were solved numerically for C_{Af} at given C_{AO} and C_{BO} employing values of the characteristic parameters of the models as determined in Section 2. The results of Potts and Amis[49] were used for the reaction velocity constant k. The numerical techniques involved, the computer program description as well as a comparison between the results for the two models are presented

in Appendix 2.3. It was found that the models predicted almost identical results in the range of parameters used, model A giving a slightly higher value for C_{Af} / C_{AO} Due to this close agreement a single line is used in Figs.11, 12 and 13 to represent both models when comparing these results with those determined experimentally.

3.4 EXPERIMENTAL RESULTS AND DISCUSSION

The experimental results are tabulated below and presented graphically in Figs. 11, 12 and 13.

TABLE 13

RUN NO.	$\bar{u}$ (cm/sec)	L (cms)	TEMP. (°C)	C_{AO} (g.moles /litre)	C_{BO} (g.moles / litre)	C_{Af} (g.moles /litre)	$\frac{C_{Af}}{C_{AO}}$
1		38	22.3	.1100	.3001	.0797	.725
2		84	22.3	.1100	.3000	.0561	.510
3	3.1	130	22.3	.1097	.2998	.0400	.365
4		175	22.3	.1098	.2999	.0296	.270
5		221	22.3	.1098	.2998	.0220	.200

RUN NO.	$\bar{u}$ (cm/sec)	L (cms.)	TEMP. (°C)	C_{AO} (g.moles /litre)	C_{BO} (g.moles /litre)	C_{Af} (g.moles /litre)	$\frac{C_{Af}}{C_{AO}}$
6		38	22.3	.1098	.2998	.0762	.694
7		84	22.3	.1095	.2996	.0509	.465
8	2.7	130	22.3	.1090	.2992	.0349	.320
9		175	22.3	.1094	.2995	.0250	.229
10		221	22.3	.1097	.2998	.0180	.164
11		38	22.3	.1098	.2999	.0710	.647
12		84	22.3	.1097	.2997	.0442	.403
13	2.2	130	22.3	.1095	.2996	.0284	.259
14		175	22.3	.1090	.2992	.0186	.171
15		221	22.3	.1093	.2994	.0126	.115
16		38	21.9	.1688	.2887	.1260	.746
17		84	22.0	.1682	.2882	.0920	.547
18	3.1	130	22.2	.1684	.2886	.0699	.415
19		175	22.3	.1682	.2882	.0543	.323
20		221	22.3	.1678	.2880	.0427	.254
21		38	21.8	.1683	.2883	.1211	.720
22		84	22.0	.1682	.2882	.0853	.507
23	2.7	130	22.1	.1680	.2880	.0632	.376
24		175	22.3	.1682	.2884	.0480	.285
25		221	22.3	.1676	.2879	.0366	.218

RUN NO.	$\bar{u}$ (cm/sec)	L (cms)	TEMP. (°C)	C_{AO} (g.moles /litre)	C_{BO} (g.moles /litre)	C_{Af} (g.moles /litre)	$\frac{C_{Af}}{C_{AO}}$
26		38	21.7	.1678	.2876	.1129	.673
27		84	21.9	.1680	.2879	.0760	.452
28	2.2	130	22.1	.1680	.2880	.0530	.315
29		175	22.2	.1682	.2881	.0387	.230
30		221	22.3	.1674	.2876	.0279	.167
31		38	25.7	.1672	.5520	.0908	.543
32		84	25.7	.1669	.5518	.0412	.247
33		130	25.7	.1668	.5518	.0214	.128
34		175	25.7	.1660	.5511	.0095	.057
35		221	25.7	.1654	.5506	.0045	.027
36		38	25.7	.1666	.5517	.0825	.495
37		84	25.7	.1663	.5516	.0345	.207
38	2.7	130	25.7	.1668	.5520	.0172	.103
39		175	25.7	.1664	.5513	.0097	.058
40		221	25.7	.1650	.5499	.0025	.015
41		38	25.7	.1672	.5522	.0714	.427
42		84	25.7	.1664	.5517	.0258	.155
43	2.2	130	25.7	.1660	.5510	.0087	.052
44		175	25.7	.1665	.5517	.0050	.030
45		221	25.7	.1660	.5514	.0017	.010

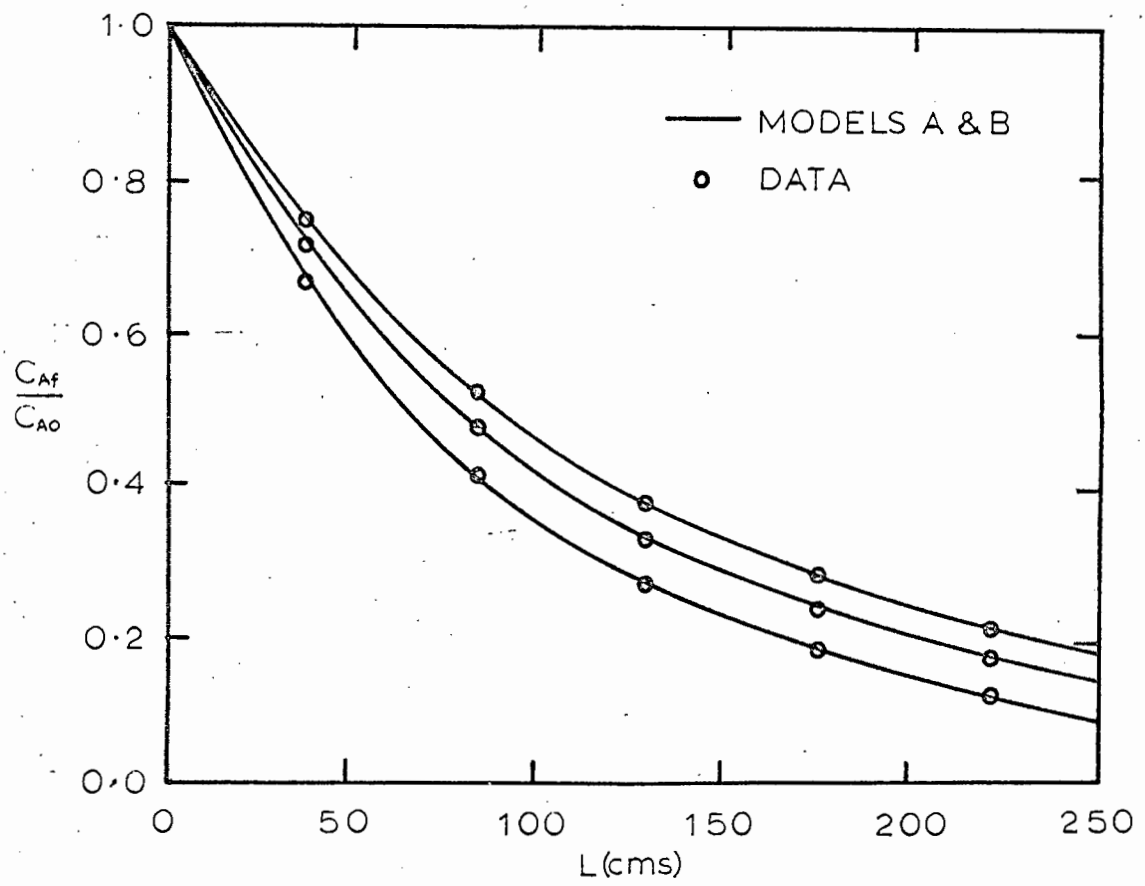

FIGURE 11 RUN NOS. 1–15

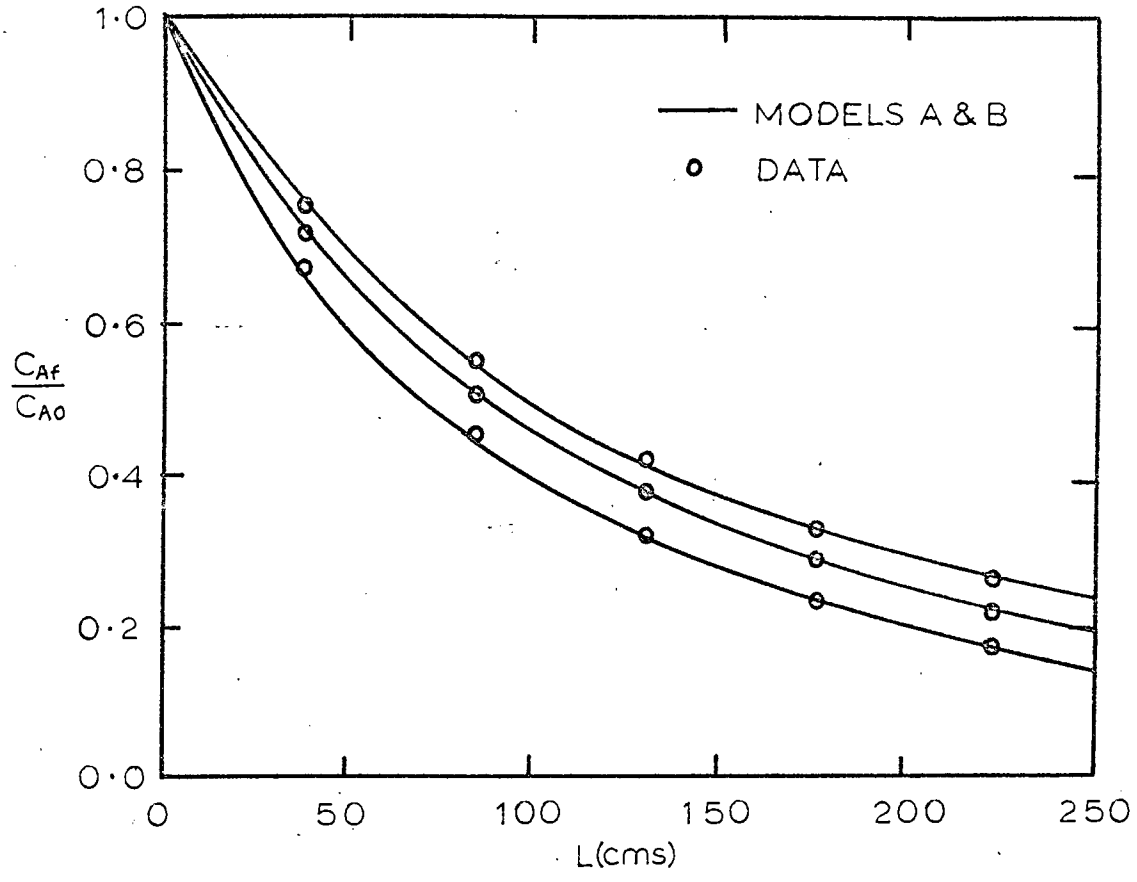

FIGURE 12 RUN NOS. 16-30

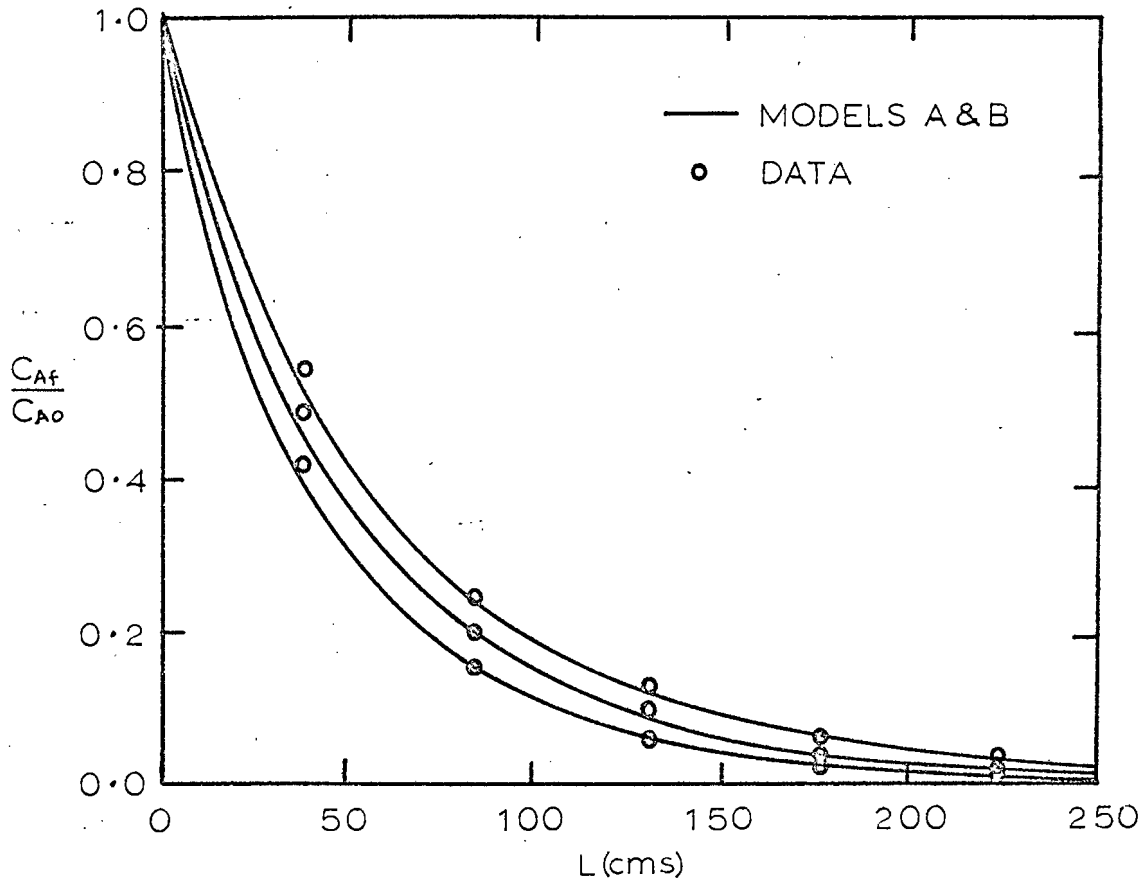

FIGURE 13 RUN NOS. 31 – 45

It can be seen that very good agreement exists between experiment and theory apart from a few results in Fig.13. Here the experimental values of C_{Af}/C_{AO} are slightly higher than those predicted by the models. This tendency leads one to show some preference for model A (See Appendix 2.3), however, it should be borne in mind that the concentrations of the reactants used in runs 31 to 45 were such that experimental errors would be expected to be higher than in the previous runs.

3.5 CONCLUSIONS

The use of a second order chemical reaction to confirm postulated flow mechanisms has been demonstrated. The application of the technique to the liquid side in a packed bed presented a number of analytical difficulties. On account of the close degree of approach to plug flow and the small residence times involved, a fast reaction had to be performed to enable the non-plug flow behaviour to be sufficiently detectable. Extreme care had to be exercised to eliminate time lags in the inlet and measuring systems. From the results presented in this section it is fairly evident that the procedure finally adopted fulfilled these requirements.

It has been shown that the theoretical values for Models A and B are very similar - the differences being smaller than the expected experimental error. For this reason it is impossible to say with certainty which model fits the data to a closer degree. This is to be expected, however, as it can be postulated that a Model A stream is equivalent to a Model B stream with the effective coefficient of axial diffusivity D_r taking into account the velocity profile and

mixing regions. This can be approached in a similar fashion to the theoretical analyses of Taylor[32-34] and other workers.[35-38]

Nomenclature for Section 3.

C_A	-	concentration of A, i.e. ethyl acetate.
C_B	-	concentration of B, i.e. sodium hydroxide.
C_{AO}, C_{BO}	-	initial concentrations of A and B resp.
C_{Af}, C_{Bf}	-	final concentrations of A and B resp.
C_{Be}	-	equilibrium concentration of B
C_{AX}, C_{AZ}	-	concentration of A in samples X and Z resp.
C_{BW}, C_{BY}	-	concentration of B in samples W and Y resp.
D	-	effective axial diffusion coefficient for entire bed
D_r	-	effective axial diffusion coefficient for r th stream.
E (t)	-	external age distribution function.
k	-	second order reaction velocity constant.
k'	-	first order reaction velocity constant.
L	-	height of packing.
r	-	rate of reaction.
$\bar{u}$	-	Mean axial velocity of liquid in bed.
u	-	point axial velocity of liquid in film.
V_w	-	flow rate of Sample W
V_x	-	flow rate of sample X
V_y	-	flow rate of sample Y
V_z	-	flow rate of sample Z
x	-	axial distance from top of bed.

BIBLIOGRAPHY

1 Danckwerts, P.V., A.I.Ch.E. Journal, 1955, 1, 456.

2. Danckwerts, P.V. & Kennedy, A.M., Trans. Instn.Chem.Engrs., 1954, 32, S 49.

3. Yoshida, F. & Koyanagi, T., A.I. Ch.E. Journal, 1962, 8, 305.

4. Onda, K., Sada, E. and Murase, Y., A.I.Ch.E. Journal, 1959, 5, 235.

5. Thomas, W.J., Trans. Instn. Chem. Engrs., 1964, 42, 3.

6. Shulman, H.L. et al., A.I.Ch.E. Journal, 1960, 6, 174

7. Norman, W.S. & Sammak, F.Y.Y., Trans. Instn.Chem.Engrs., 1963, 41, 109

8. King, R.P., M.Sc. Thesis, 1962, University of the Witwatersrand.

9. King, R.P., Reactor, 1963, 2, 23

10. Davidson, J.F., Trans. Instn. Chem. Engrs., 1959, 37, 131

11. Shulman, H.L. et al., A.I.Ch.E. Journal, 1955, 1, 253

12. Whitt, F.R., Brit. Chem. Engng., 1956, 1, 437

13. Mada, J. et al., Kagaku Kogaku, 1964, 2, 111

14. Danckwerts, P.V., Trans. Instn. Chem. Engrs., 1959, 37, 147

15. Danckwerts, P.V. et al., Chem. Engng.Sci., 1963, 18, 63

16. Sherwood, T.K. & Holloway, F.A.L., Trans. Amer. Inst. Chem. Engrs., 1940, 36, 39.

17. Cooper, C.M. et al., Trans. Amer. Inst. Chem. Engrs., 1941, 37, 979

18. Sherwood, T.K. & Pigford, R.L., "Absorption and Extraction", 1952, (New York : McGraw-Hill Book Co.Inc.)

19. Perry, J.H., "Chemical Engineers Handbook", 1964, (New York : McGraw-Hill Book Co. Inc.)

20. Danckwerts, P.V., Chem. Engng. Sci., 1953, 2, 1.

21. Glaser, M.B., & Lichtenstein, I., A.I.Ch.E. Journal, 1963, 9, 30.

22. Mori, Y. et al., Kagaku Kogaku, 1964, 2, 173

23. Carberry, J.J. & Bretton, R.H., A.I. Ch.E. Journal, 1958, 4, 367

24. James, H., M.Sc. Thesis, 1964, University of the Witwatersrand

25. Lapidus, L. & Amundson, N.R., J.Phys.Chem., 1952, 56, 984.

26. McHenry, K.W. & Wilhelm, R.H., A.I.Ch.E. Journal, 1957, 3, 83.

27. Strang, D.A. & Geankoplis, L.J., Industr. Engng. Chem., 1958, 50, 1305.

28. Ebach, E.A. & White, R.R., A.I. Ch.E. Journal, 1958, 4, 161

29. Everson, R.C., M.Sc. Thesis, 1965, University of Natal

30. Levenspiel, O., "Chemical Reaction Engineering", 1962, (New York : John Wiley & Sons , Inc.)

31. Ceaglske, N.H., "Automatic Process Control for Chemical Engineers", 1956, (New York : John Wiley & Sons, Inc.)

32. Taylor, G.I., Proc. Roy. Soc., 1953, A219, 186

33. Taylor, G.I., Proc. Roy. Soc., 1954, A223, 446

34. Taylor, G.I., Proc. Roy.Soc., 1955, A225, 473

35. Aris, R., Proc. Roy.Soc., 1956, A235, 67

36. Aris, R., Proc.Roy.Soc., 1959, A252, 538

37. Bailey, H.R. & Gogarty, W.B., Proc.Roy.Soc., 1962, A269, 352

38. Tichacek, L.J. et al., A.I. Ch.E. Journal, 1957, 3, 439

39. Aris, R., Proc. Roy. Soc., 1960, A259, 370

40. Hull, D.E. & Kent, J.W., Industr. Engng. Chem., 1952, 44, 2745

41. Lee, J.C., Chem. Engng. Sci., 1960, 12, 191

42. Davidson, J.F. et al., Chem. Engng. Sci., 1955, 4, 201

43. Cairns, E.J. & Prausnitz, J.M., Chem. Engng. Sci., 1960, 12, 20

44. Turner, G.A., Chem. Engng. Sci., 1958, 7, 156

45. Glaser, M.B. & Litt, M., A.I.Ch.E. Journal, 1963, 9, 103

46. Otake, T. & Kunugita, E., Chem. Eng. (Japan), 1958, 22, 143

47. Wehner, J.F. & Wilhelm, R.H., Chem.Engng.Sci., 1956, 6, 89

48. Wang, Y.L. & Longwell, P.A.I A.I. Ch.E. Journal, 1964, 10, 323

49. Potts, J.E. & Amis, E.S., J. Amer. Chem. Soc., 1949, 71, 2112

50. Asbjornsen, O.A., Chem. Engng. Sci., 1961, 14, 211

51. Bryson, A.W., Reactor, 1965, 3, 39

52. Bird, R.B., Stewart, W.E. & Lightfoot, E.N., "Transport Phenomena", 1963, (New York : John Wiley & Sons, Inc.)

53. Bryson, A.W., Reactor, 1962, 1, 19

APPENDIX 1

1.1 Fitting of tail of residence time distribution curve to a logarithmic decay function.

The tail of the curve was fitted to the equation:

$$f(t) = Ae^{-Rt}$$

The plot of log. f(t) against t was found to approximate to a straight line for all the residence time distribution curves at $t \geq \tau^*$. The examples tabulated below have been taken from a series of runs with a packed height of 114 cms. at the four water rates used. The results are also presented graphically in Fig. 14.

TABLE 14.

Run No.17 L = 114 cms. W = 15.4 ml/sec. τ^* = 68 secs.		Run No. 21 L = 114 cms. W = 20.2 ml/sec. τ^* = 54 secs.		Run No. 25 L = 114 cms. W = 26.2 ml/sec. τ^* = 46 secs.		Run No. 29. L = 114 cms. W = 33.6 ml/sec. τ^* = 38 secs.	
t(secs)	log f(t)	t(secs)	log f(t)	t(secs)	log f(t)	t(secs)	log f(t)
68	1.00	54	1.08	46	1.02	38	1.14
70	.92	56	.99	48	.90	40	1.01
72	.86	58	.90	50	.79	42	.89
74	.79	60	.81	52	.69	44	.76
76	.72	62	.72	54	.58	46	.62
78	.64	64	.60	56	.46	48	.52

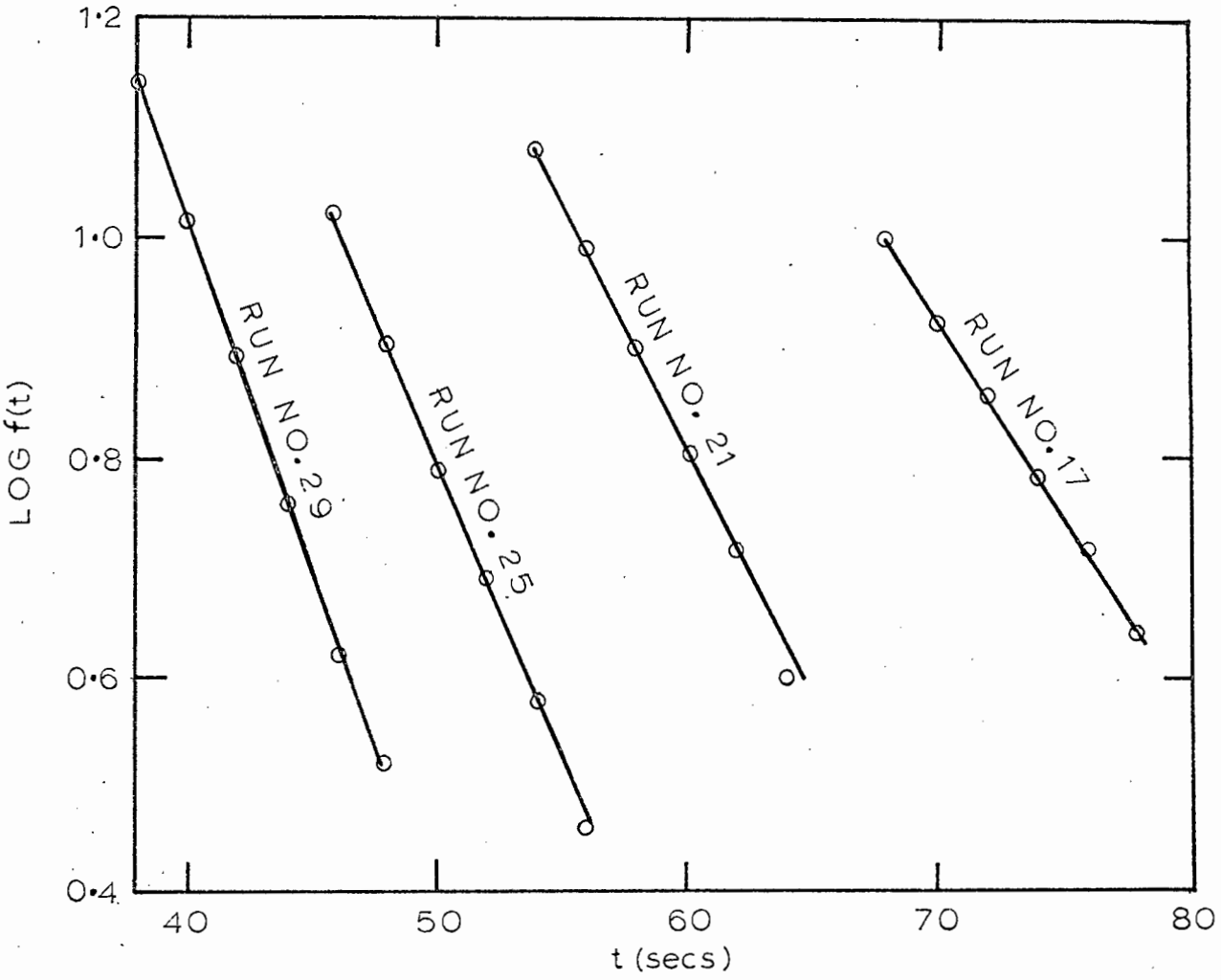
1·2
1·0
0·8
0·6
0·4
LOG f(t)
40
50
60
70
80
t (secs)
RUN NO. 29
RUN NO. 25
RUN NO. 21
RUN NO. 17

FIGURE 14

1.2 Development of the velocity profile in a laminar film.

Values of $\frac{u(x,y)}{\bar{u}}$ computed from equation (2.117) are compared with those reported in the literature.[48]

TABLE 15

Z	y	$u(x,y)/\bar{u}$ Equation (2.117)	Schlichting	Wang & Longwell
	0.95	0.774	0.705	0.828
	0.9	0.889	1.007	0.996
	0.8	0.959	1.040	1.032
	0.7	0.985	1.040	1.027
	0.6	0.998	1.040	1.021
0.05	0.5	1.006	1.040	1.018
	0.4	1.010	1.040	1.016
	0.3	1.014	1.040	1.014
	0.2	1.016	1.040	1.013
	0.1	1.017	1.040	1.013
	0.0	1.017	1.040	1.012
	0.95	0.461	0.399	0.426
	0.9	0.666	0.720	0.762
	0.8	0.854	1.046	1.062
0.20	0.7	0.942	1.088	1.105
	0.6	0.992	1.088	1.094
	0.5	1.023	1.088	1.081
	0.4	1.043	1.088	1.071

Z	y	$u(x,y)/\bar{u}$ Equation (2.117)	Schlichting	Wang & Longwell
	0.3	1.057	1.088	1.065
	0.2	1.065	1.088	1.061
0.20	0.1	1.070	1.088	1.059
	0.0	1.071	1.088	1.058
	0.95	0.255	0.245	0.217
	0.9	0.444	0.467	0.425
	0.8	0.701	0.806	0.788
	0.7	0.867	1.082	1.030
	0.6	0.980	1.130	1.148
0.50	0.5	1.059	1.182	1.189
	0.4	1.115	1.192	1.197
	0.3	1.154	1.196	1.195
	0.2	1.180	1.196	1.191
	0.1	1.195	1.196	1.189
	0.0	1.200	1.196	1.189
	0.95	0.176	0.172	0.171
	0.9	0.333	0.333	0.332
	0.8	0.595	0.619	0.618
0.80	0.7	0.803	0.858	0.855
	0.6	0.968	1.041	1.039
	0.5	1.098	1.175	1.172
	0.4	1.198	1.265	1.259

	0.3	1.272	1.317	1.311
	0.2	1.324	1.338	1.340
0.80	0.1	1.354	1.346	1.353
	0.0	1.364	1.347	1.357
	0.95	0.160	0.156	0.154
	0.9	0.307	0.302	0.300
	0.8	0.566	0.568	0.564
	0.7	0.783	0.797	0.793
	0.6	0.964	0.989	0.985
0.90	0.5	1.111	1.143	1.140
	0.4	1.228	1.261	1.260
	0.3	1.317	1.347	1.347
	0.2	1.379	1.404	1.406
	0.1	1.416	1.436	1.440
	0.0	1.429	1.446	1.451

1.3 Moments of input and output signals for single outlet column runs.

In the first set of data, i.e. run numbers 1 to 16, the mean residence time of the input curve was used as the time origin. For the remaining runs an arbitrary point ahead of the breakaway time of the input curve was selected as origin.

TABLE 16

All values of T_m expressed in seconds, T_s^2 in (seconds)^2 and T_a^3 in (seconds)^3.

RUN	INPUT			OUTPUT		
No.	T_m	T_s^2	T_a^3	T_m	T_s^2	T_a^3
1	0.0	2.8	9.3	54.3	160	2119
2	0.0	2.7	9.0	39.7	112	1389
3	0.0	2.8	9.7	32.3	91	1140
4	0.0	2.8	9.0	16.9	55	699
5	0.0	2.0	4.9	45.4	100	1065
6	0.0	2.0	5.3	32.8	66.6	540
7	0.0	2.0	5.5	26.6	52.7	428
8	0.0	2.1	6.0	14.6	31.3	242
9	0.0	0.83	1.4	37.5	59.0	369
10	0.0	0.87	1.5	27.3	40.8	211
11	0.0	0.79	1.3	22.3	33.6	169
12	0.0	0.80	1.5	12.6	18.8	91
13	0.0	0.52	1.1	32.6	43.5	194
14	0.0	0.50	0.9	23.1	29.9	124
15	0.0	0.48	0.9	19.0	23.9	101
16	0.0	0.42	0.8	10.0	13.4	57
17	2.2	2.9	10.0	56.5	169	2776
18	2.1	2.9	9.1	42.0	115	1650
19	2.1	3.0	10.3	34.3	91.5	1426
20	2.2	3.1	10.1	19.2	50.5	698
21	1.6	2.1	5.3	47.5	105	1426
22	1.7	2.4	6.4	34.7	69.2	672
23	1.6	2.1	5.0	28.6	54.5	585

RUN No.	INPUT			OUTPUT		
	T_m	T_s^2	T_a^3	T_m	T_s^2	T_a^3
24	1.8	2.4	6.0	16.3	30.1	290
25	1.3	.99	1.5	39.8	66.5	666
26	1.3	.89	1.8	29.0	45.0	302
27	1.4	.92	2.3	24.5	37.3	286
28	1.3	.90	1.9	13.5	20.0	131
29	1.0	.55	1.0	35.3	39.9	264
30	1.0	.52	1.0	24.5	30.0	192
31	1.0	.61	1.2	20.4	24.6	121
32	1.0	.50	0.7	11.3	13.2	55.5
33	2.4	3.0	10.2	57.3	179	2880
34	2.0	2.9	9.7	42.6	123	1901
35	2.6	3.3	11.3	35.1	101	1699
36	2.0	2.8	9.0	19.4	54.7	730
37	1.9	2.2	5.6	48.7	92.8	958
38	1.7	2.3	6.6	35.0	72.0	704
39	1.7	2.1	5.0	29.6	56.3	616
40	1.7	2.1	5.3	16.8	31.0	305
41	1.3	0.88	1.5	40.4	76.2	765
42	1.3	0.97	2.0	29.4	46.4	336
43	1.6	0.80	1.3	25.2	40.2	303
44	1.3	0.83	1.8	13.9	22.2	141
45	1.0	0.57	1.3	35.5	41.0	288
46	0.9	0.47	0.8	25.0	33.7	207
47	1.2	0.54	1.0	21.3	25.8	158
48	1.0	0.48	1.0	11.4	13.7	63.3

1.4 Values of ϕ as plug flow is approached.

$$\phi = \frac{T_m T_a^3}{T_s^4}$$

For true plug flow the value of ϕ is indeterminate, as $T_a^3 = 0$ and $T_s^4 = 0$. As this condition is approached ϕ tends to widely different values depending on the nature of the distribution curve. Two examples are given below:

(a) For a series of n mixed tanks each with time constant T,

$$G(s) = \frac{1}{(Ts + 1)^n}$$

giving $T_m = n T$

$T_s^2 = n T^2$

$T_a^3 = 2nT^3$

$\therefore \phi = 2$ for all n

As $n \to \infty$ the system tends to plug flow, however, the value of ϕ is still equal to 2.

(b) For a flow situation which can be described by a dead time T_1 and a backmix region with time constant T_2,

$$G(s) = \frac{e^{-T_1 s}}{T_2 s + 1}$$

$$T_m = T_1 + T_2$$

$$T_s^2 = T_2^2$$

$$T_a^3 = 2T_2^3$$

$$\phi = 2\,(T_1/T_2 + 1)$$

As plug flow is approached $T_2 \rightarrow 0$,

hence $\phi \rightarrow \infty$

APPENDIX 2

Note: Machine print-out copies of the computer programs have not been presented in this appendix as a number of the symbols contained on the printer of the I.C.T. 1301 used do not conform to the Manchester Auto-Code.

2.1 Moment analysis program.

The contribution of the first half of the curve to each of the moments about τ^* was determined by integration according to the trapezium rule. This was performed in Chapter O, where the variables B, C, D and E were the contributors to the zero, first, second and third moments respectively. In Chapter 1 the moments about τ^* were computed for times greater than τ^*. Here the curve was assumed to fit an exponential decay function. (see Appendix 1.1). The two contributors were then added and normalised. Chapter 2 transfers the first moment to the origin and the second as well as the third to the mean residence time.

The M.A.C. program used was as follows:

```
CHAPTER 1
A → 80
1) READ (X)
X = φ LOG (X)
Y = φ LOG (AT)
```

```
Z = φ DIVIDE (N, Y-X)
B = B - .5AT + ZAT
C = C + ZZAT
D = D + 2ZZZAT
E = E + 6ZZZZAT
C = SC/B
D = SSD/B
E = SSSE/B
UP
CLOSE
CHAPTER 2
VARIABLES 1
2) PRINT 'RUN NUMBER'
PRINT (W) 4,0
NEWLINE
PRINT 'FM'
PRINT (C + ST) 4,4
NEWLINE
PRINT 'SM'
PRINT (D-CC) 4,4
NEWLINE
PRINT 'TM'
PRINT (E - 3CD + 2CCC) 4,4
NEWLINE
F = C + ST
G = D - CC
H = E - 3CD + 2CCC
```

```
G = φ SQRT(G)
F =  G/F
PRINT 'GAMMA 1'
PRINT (F) 2,4
NEWLINE
H = φ DIVIDE (H, GGG)
PRINT 'GAMMA 2'
PRINT (H) 2,4
NEWLINE
H = H/F
PRINT 'GAMMA RATIO'
PRINT (H) 2,4
NEWLINE 2
UP
CLOSE.
CHAPTER O
VARIABLES 1
1)READ (W)
JUMP 4, W = 0
READ (M)
READ (T)
READ (S)
READ (N)
I = M - 1
2) I = I + 1
READ (AI)
JUMP 3, I = T
JUMP 2
```

```
3) B = 0
C = O
D = O
E = O
I = M (I) T
B = B + AI
C = C + IAI - TAI
D = D + IIAI - 2ITAI + TTAI
E = E + IIIAI - 3IITAI + 3ITTAI - TTTAI
REPEAT
DOWN 1/1
DOWN 2/2
JUMP 1
4) END
CLOSE.
```

A typical data card for this program read as follows:

19 10 20 2 4 19 84 163 233 272 271 250 213 180 143 113 46.

This set of data gave the print out:

```
RUN NUMBER 19
F M   34.3272
S M   91.5077
T M   1426.3953
GAMMA 1    0.2787
GAMMA 2    1.6295
GAMMA RATIO   5.8474
```

2.2 Model B Program

B_1 , B_2 and B_3 were evaluated by integration of equations 2.142, 2.143 and 2.144 according to the trapezium rule for values of Z' from 0.3 upwards in steps of 0.001. The value of $\frac{B_1 B_3}{B_2^2}$ was also recorded.

The main program variables used mere:

Z for Z'
A for B_1
D for B_2
E for B_3
U for $u(x,y) / \bar{u}$

The M.A.C. program read as follows:

```
CHAPTER 1
U → 40
A → 40
B → 40
C → 40
U = .025 U
A = .025 A
B = .025 B
C = .025 C
D = B - AA
E = C - 3AB + 2AAA
PRINT (2) 1,4
V = φ DIVIDE (AE,DD)
```

```
PRINT (V) 2,
PRINT (V) 1, 4
PRINT (A) 1,4
PRINT (D) 1, 5
PRINT (E) 1,6
NEWLINE
ACROSS 1/0
CLOSE
CHAPTER 0
VARIABLES 1
Z = .3
1) Z = Z + .001
I = 0(1) 39
Y = .025 I
H = 1.5 - 1.5 YY
H = 1 - 1/H
G = φ DIVIDE (1 - HZ, 1 - Z)
F = φ LOG (1 - Z)
G = G - HF - 1
U = φ DIVIDE (1, 1 - HZ)
UI = U
AI = UG
BI = UGG
CI = UGGG
REPEAT
U = .5UO
```

```
A    =   .5AO
B    =   .5BO
C    =   .5CO
I    =   1(1)39
U    =   U + UI
A    =   A + AI
C    =   C + CI
REPEAT
CLOSE.
```

A number of the results obtained are tabulated below:

TABLE 17.

Z'	B_1	B_2	B_3	B_1B_3/B_2^2
.370	.5655	.04536	.010569	2.9049
.380	.5903	.05042	.013971	3.2439
.390	.6159	.05599	.018203	3.5766
.400	.6424	.06211	.023436	3.9031
.410	.6698	.06883	.029878	4.2236
.420	.6981	.07623	.037777	4.5383
.430	.7275	.08437	.047425	4.8473
.440	.7580	.09332	.059175	5.1507
.450	.7896	.10317	.073445	5.4484
.460	.8224	.11401	.090736	5.7407

2.3 Numerical solutions to equations 3.9 and 3.10

The boundary conditions for equation 3.9 are:

$$C_A = C_{AO} \quad \text{at} \quad x = 0$$

$$\frac{\partial C_A}{\partial x} = O \quad \text{as} \quad x \to \infty$$

On account of the second boundary condition the Runge-Kutta method did not prove satisfactory. Since in all the runs performed the concentration of B was greater than A, equation 3.9 can be linearised over a small increment Δx as follows.

$$D \frac{d^2 C_A}{dx^2} - \bar{u} \frac{d C_A}{dx} - k C_A (C_B)_{\text{average}} = O$$

where $(C_B)_{\text{average}}$ was taken as the arithmetic mean concentration of B over the increment. The solution to the above equation is as for a first order reaction, i.e.,

$$\frac{C_A (x + \Delta x)}{C_A (x)} = \exp\left[\frac{\bar{u} \Delta x}{2D} - \sqrt{\frac{\bar{u}^2 (\Delta x)^2}{4D^2} + \frac{k (C_B)_{\text{average}} (\Delta x)^2}{D}}\right]$$

Commencing at a large value of x where a value of C_A is assumed, calculations are performed for each increment up the curve until the point $x = 0$ is reached. At this stage the current value of C_A is compared with the required value of C_{AO} and if the discrepancy is too large the procedure is repeated with a new assumed value of C_A at the initial value of x.

The M.A.C. program used was:

```
CHAPTER 1
Y       →       150
7) PRINT (D) 1,4
PRINT (B) 1,2
PRINT (C) 1,4
NEWLINE
E       =  ϕ    EXP (300 C B)
E       =  ϕ    DIVIDE (E, 1 - B)
Y150    =  ϕ    DIVIDE (BE, E-1)
T       =       O
4) Z    =       O
X       =       Y150
P       =       149 (-1) O
I       =       O
1 ) H   =  ϕ    SQRT (DD + 2CDX - 2CDB)
I       =       I + 1
H       =  ϕ    EXP (2H - 2D)
YP      =       HY (P + 1)
Z       =       X
X       =       YP/2 + Y (P + 1) / 2
Z       =       Z - X
Z       =       ZZ
JUMP 1, Z>.000000005
JUMP 1, I = 1
2) REPEAT
```

```
JUMP 10, YO > 1.0001
JUMP 3,   T = 1
Y150  =   Y150 + .001
JUMP 4
10) Y150 = Y150 - .0001
T = 1
JUMP 4
3) ACROSS 3/0
CLOSE
CHAPTER O
VARIABLES 1
8) NEWLINE 5
READ (D)
READ (C)
ACROSS 7/1
3) N = 10 (10) 150
PRINT (2N) 3,0
PRINT (YN) 1,4
NEWLINE
REPEAT
STOP 1155
JUMP 8
CLOSE.
```

To solve equation 3.10, the film was divided into 40 layers of equal thickness. The concentration of reactant A was evaluated after length of film x', 2x', etc., assuming plug flow in each layer. At each mixing section a mass balance was

performed to determine the average concentration of A, which in turn became the initial concentration for the next length of film.

M.A.C. program:

```
CHAPTER 1
A → 40
G → 40
W → 40
1) A = .025 A
B = A - A' + B'
N = N + 1
PRINT (NX) 3,2
PRINT (A) 1,4
PRINT (B) 1,4
F = φ DIVIDE (AE, BD)
F = φ LOG (F)
F = φ DIVIDE (FV, NXH'D - NXH'E)
PRINT (F) 1,4
PRINT (NXF) 3,2
A' = A
B' = B
UP
CLOSE
CHAPTER 0
VARIABLES 1
1) NEWLINE 3
READ (D)
```

```
READ (E)
READ (H')
READ (Z)
READ (X)
READ (V)
A'    =  D
B'    =  E
N     =  O
2) NEWLINE
W     =  O
I     =  O (1) 39
Y     =  .025 I
H     =  1.5 - 1.5 YY
H     =  1 - 1/H
Z'    =  1 - Z
F     =  φ LOG (Z')
G     =  1/Z' - HZ/Z' - HF - 1
GI    =  GZ'/Z
WI    =  I/GI
W     =  W + WI
REPEAT
A     =  O
I     =  O (1) 39
G     =  .025GIWX/V
U     =  40 WI/W
G     =  φ EXP (GH'A' - GH'B')
AI    =  φ DIVIDE (A'G - B'G, G - B'/A')
```

```
A                    A    =   A + Al
                     REPEAT
                     DOWN 1/1
                     JUMP 3, 21 SET
                     JUMP 2
                     3) END
                     JUMP 1
                     CLOSE.
```

A comparison between some of the results obtained for the two models is given below.

TABLE 18

PARAMETERS	Bed Height L (cms.)	C_A/C_{AO}	
		Model A	Model B
$\bar{u}$ = 2.2 cm/sec	35	.667	.663
x' = 35.0 cms	70	.461	.458
k = .0941 litres/g. mole sec.	105	.328	.325
	140	.238	.235
C_{AO} = 0.1100 g.moles/litre	175	.175	.172
C_{BO} = 0.3001 g.moles/litre	210	.129	.126
	245	.096	.094
$\bar{u}$ = 2.2 cm/sec	35	.425	.407
x' = 35.0 cms.	70	.196	.185
k = .1183 litres/g.mole sec.	105	.095	.088
C_{AO} = 0.1660	140	.047	.043
	175	.023	.020
C_{BO} = 0.5511	210	.012	.010
	245	.006	.005